High mid-Holocene accumulation rates over West Antarctica inferred from a pervasive ice-penetrating radar reflector

Julien A. Bodart[1], Robert G. Bingham[1], Duncan A. Young[2], Joseph A. MacGregor[3], David W. Ashmore[4,5], Enrica Quartini[2,~~5~~6], Andrew S. Hein[1], David G. Vaughan[~~6~~7†], and Donald D. Blankenship[2]

[1]School of GeoSciences, University of Edinburgh, Edinburgh, UK
[2]Institute for Geophysics, University of Texas at Austin, Austin, Texas, USA
[3]Cryospheric Sciences Laboratory, NASA Goddard Space Flight Center, Greenbelt, Maryland, USA
[4]School of Environmental Sciences, University of Liverpool, Liverpool, UK
[5]MET Office, Exeter, UK
[6~~5~~]Department of Astronomy, Cornell University, Ithaca, New York, USA
[7~~6~~]British Antarctic Survey, Cambridge, UK
[†] Deceased

Correspondence to: Julien A. Bodart (julien.bodart@ed.ac.uk)

Key points

- We estimate mean accumulation rates for the past ~~~5000~~ 4700 years across the Pine Island, Thwaites, and Institute and Möller ice-stream catchments in West Antarctica using a ubiquitous, ice-core dated internal radar~~-sounded and ice core-dated Internal Reflecting Horizon~~ reflection
- Accumulation rates were 18% higher during the mid-Holocene compared to modern rates over the Amundsen-Weddell-Ross ~~Sea~~ divide
- Spin-up of regional and continental ice-sheet models~~Spin-up of ice-sheet models~~ ~~must~~ should ~~account~~ include~~for~~ time-varying changes in Holocene accumulation rates from the WAIS Divide Ice Core ~~between the Last Glacial Maximum and the present~~ to generate more realistic grounding-line evolution and past sea level rise contribution across this region

Abstract

~~Modelling~~ Understanding the past and future evolution of the Antarctic Ice Sheet ~~the West Antarctic Ice Sheet (WAIS) to atmospheric and ocean forcing~~ is challenged by the availability and quality of observed palaeo-boundary conditions. Numerical ice-sheet models often rely on these palaeo-boundary conditions to guide and evaluate their models' predictions of sea-level rise, with varying levels of confidence due to the sparsity of existing data across the ice sheet. A k~~K~~ey ~~potential~~ data source for large-scale ~~reconstructing~~ reconstruction of past ice-sheet processes ~~on large spatial scales~~ are Internal Reflecting Horizons (IRHs) detected by Radio-Echo Sounding (RES) ~~techniques~~. When isochronal and dated at ice cores, IRHs can be used to determine palaeo-accumulation rates and patterns therein. Using a spatially extensive IRH over Pine Island Glacier, Thwaites Glacier, and Institute and Möller Ice Streams (covering a total of 610 000 km^2 or 30% of the WAIS), and a local layer approximation model, we infer mid-Holocene accumulation rates over the slow-flowing parts of these catchments for the past ~47~~50~~00 years. By comparing our results with modern climate reanalysis models (1979–2019) and observational syntheses (1651–2010), we estimate that accumulation rates over the Amundsen-Weddell-Ross divide were on average 18% higher during the mid-Holocene than modern rates ~~during the mid-Holocene~~. However, no significant spatial changes in the accumulation pattern were observed. The~~se~~ higher mid-Holocene accumulation-rate estimates match previous palaeo-accumulation estimates from ice-core records and targeted RES surveys over the ice divide, and they also coincide with periods of grounding-line re-advance during the Holocene over the Weddell and Ross Sea sectors. We find that our spatially-extensive, mid-Holocene-to-present accumulation estimates are consistent with a sustained late-Holocene period of higher accumulation rates occurring over millennia at the WAIS Divide Ice Core, thus highlighting the spatial representativeness of this ice core to the wider West Antarctic region. ~~Our results highlight the need for ice-sheet models to account for time-varying accumulation rates across the WAIS during the Holocene to provide better estimates of its contribution to past sea-level rise.~~ We conclude that future regional and continental ice-sheet modelling studies should base their climatic forcings on time-varying accumulation rates from the WAIS Divide Ice Core through the Holocene to generate more realistic predictions of the West Antarctic Ice Sheet's past contribution to sea-level rise.

Key words: West Antarctica, Internal Reflecting Horizons, Accumulation, Holocene, Ice-Penetrating Radars, Ice-Core, Pine Island Glacier, Thwaites Glacier.

1. Introduction

Improving our knowledge of past climatic changes over the ~~West Antarctic Ice Sheet~~Antarctic Ice Sheet ~~(WAIS)~~ is required if we are to understand its present evolution and model its future under increasingly rapid climatic changes (IPCC, 2021). Most studies of past ice-sheet behaviour over Antarctica~~the WAIS~~ have focused on modelling changes in ice volume and grounding-line ~~(GL)~~ retreat following the Last Glacial Maximum (LGM, ~20 ka Before Present, BP) (Denton and Hughes, 2002; Golledge et al., 2012; 2013; Hillenbrand et al., 2013; 2014; Le Brocq et al., 2011; Kingslake et al., 2018); however, less attention has been paid to ice-sheet evolution during the Holocene (~11.7 ka BP to present). Recent evidence suggests that ~~the~~ parts of the grounding line of West Antarctica ~~GL~~ may have retreated several hundred kilometres inland from its current position at ~10 ka and subsequently re~~-~~advanced to reach its modern position sometime during the Holocene, due to isostatic rebound and climate-induced changes, particularly over the Weddell Sea and western Ross Sea sectors (Siegert et al., 2013; Bradley et al., 2015; Kingslake et al., 2018; Wearing and Kingslake, 2019; Venturelli et al., 2020; Neuhaus et al., 2021; Johnson et al., 2022). However,

~~T~~ the ~~inland~~ atmospheric and ice-dynamical conditions farther inland, which ~~may~~ could also have induced ~~have partly caused this Holocene~~ grounding-line ~~GL~~ migration, remain ~~relatively under-studied~~poorly constrained. An early investigation by Whillans (1976) using radar data near Byrd Ice Core indicated stability during the Late Pleistocene and Holocene epochs ~~and late Pleistocene~~. Records of temperature and precipitation from the WAIS Divide Ice Core (hereafter abbreviated as WD14; Fig. 1) in the central ~~WAIS~~ West Antarctic Ice Sheet (WAIS) suggest higher accumulation rates during the Holocene than ~~the~~ at present (Fudge et al., 2016), a trend that is also observed across small parts of the ~~Western divide~~Amundsen-Weddell-Ross divide (~~hereafter referred to as WD;~~ Fig. 1) near the WAIS Divide Ice Core (hereafter referred to as WD14; Fig. 1~~WD14)~~ -where isolated Radio-Echo Sounding (RES) surveys have shown 15-30% higher accumulation rates during the mid-Holocene compared to modern values (Siegert and Payne, 2004; Neumann et al., 2008; Koutnik et al., 2016).

~~At present modelling~~ Many numerical ice-sheet models~~studies~~ that aim to predict Antarctica's ~~future~~ long-term (past and future) ~~changes~~ contribution to sea-level rise~~over the WAIS~~ use past ice-sheet reconstructions from after the LGM to guide and evaluate their models (Chavaillaz et al., 2013; DeConto and Pollard, 2016; Bracegirdle et al., 2019). However, even well-used ice-sheet reconstructions assume that the ice sheet retreated continuously throughout the Holocene (e.g. RAISED Consortium, 2014), a finding that has been challenged recently for the WAIS (e.g. Kingslake et al., 2018). ~~However~~Further, significant discrepancies between model simulations and the palaeo-proxy record currently impede our ability to predict confidently how the ice sheet will respond to future changes in the climate (e.g. Johnson et al., 2021). While improvements in model ~~physics~~ parameterisations ~~and parameterisations~~ are needed to close this gap (Bracegirdle et al., 2019; Sutter et al., 2021), ~~a~~ considerable improvement in the availability and quality of palaeo-proxy records, particularly during the Holocene, is also needed to provide better constraints for ice-sheet models and ultimately ~~gain~~ better resolve ~~a more accurate picture of the~~ past ice-sheet changes (Kingslake et al., 2018; Jones et al., 2022). Palaeo-proxy data ~~over the WAIS~~ have traditionally come from point-based measurements, such as ice cores (e.g. Petit et al., 1999; Parrenin et al., 2007; WAIS Divide Project Members, 2013; ~~; Cuffey et al., 2016; McConnell et al., 2017;~~ Buizert et al., 2021), sediment cores (e.g. Hillenbrand et al., 2013; Arnd et al., 2017; Hillenbrand et al., 2017; Kingslake et al, 2018; Venturelli et al., 2020; Neuhaus et al., 2021; Sproson et al., 2022), or ~~from~~ surface-exposure dating (e.g. Stone et al., 2003; Suganuma et al., 2014; Johnson et al., 2014; Hein et al., 2016; Nichols et al., 2019; Johnson et al., 2020; Braddock et al., 2022).

A complimentary and spatially extensive alternative data source for inferring past climate across an ice sheet is provided by Internal Reflecting Horizons (IRHs) detected by RES. They primarily result from englacial acidity contrasts ~~sounded by RES~~ and are often detected horizontally for hundreds of kilometres on RES data ~~can be traced horizontally across large parts of the ice sheet on RES profiles~~ (Harrison, 1973; Bingham and Siegert, 2007)~~, thus making them a useful resource to infer past climates on regional to continental scales (Bingham and Siegert, 2007; Harrison, 1973)~~. When employed in combination with ice-core stratigraphies~~y~~, IRHs can be used to ~~extrapolate~~ extend age-depth relationships ~~across large spatial scales~~away from an ice core by following peaks in electromagnetic power in the radar data (e.g. Beem et al., 2021; Bodart et al., 2021a; Cavitte et al., 2016; Jacobel and Welch, 2005; MacGregor et al., 2015; Whillans, 1976; Winter et al., 2019).

In ~~comparison~~ contrast to East Antarctica and Greenland, ~~extrapolating~~ IRH extension of ~~past ice-sheet records from~~ WAIS ice cores ~~to entire glacier catchments~~ has so far been challenging due to ~~the limited availability of~~fewer deep ice cores there and, until recently, the lack of ~~suitable~~ well-dated IRH datasets. However, efforts have intensified in recent years to improve our understanding of ~~the~~ ice stratigraphy over this sector. In particular, four recent studies using airborne RES data ~~over the WAIS~~ (Karlsson et al., 2014; Muldoon et al., 2018; Ashmore et al., 2020a; Bodart et al., 2021a) all identified a ~~particularly~~ distinct and bright IRH ~~precisely~~ dated using the Byrd and WD14 ice-core chronologies ~~at~~ to 4.72 ± 0.28 ka BP (Muldoon et al., 2018; Bodart et al., 2021a). A ~~C~~comparison ~~with~~ of volcanic sulphate deposition within the WD14 and Siple Dome ice cores revealed a large peak in sulphate concentration matching the age and depth of this ubiquitous ~~layer~~ IRH (Kurbatov et al., 2006; Bodart et al., 2021a; Cole-Dai et al., 2021; Sigl et al., 2022), which ~~is~~ we hereafter term~~ed~~ the "4.72 ka IRH". This IRH has now been observed by multiple RES systems ~~from different surveys and data providers. It~~and extends throughout much of the slower-flowing ice of the Amundsen and Weddell Sea embayments (< 400 m a^{-1}), including across the divides demarcating regions draining into the Amundsen, Weddell and Ross Seas.

Despite their potential wide-ranging applications, the incorporation of IRHs into ice-sheet models has so far been limited compared to other types of palaeo-proxy data, primarily because the inference of accumulation-rate or ice-flow history from IRHs is an ill-posed inverse problem (Waddington et al., 2007). Previous applications using IRHs to inform regional and continental models include: (a) constraining decadal-scale Surface Mass Balance (SMB) estimates from atmospheric models using annually-resolved IRHs found in the shallow firn (Medley et al., 2013; 2014; Van Wessem et al. 2018; Dattler et al., 2019; Kaush et al., 2020; Cavitte et al., 2022); (b) inferring past accumulation rates going back further in time (i.e. 100s to 1000s years) with the aim of comparing past accumulation estimates with modern times (e.g. Leysinger Vieli et al., 2004; Siegert and Payne, 2004; Neumann et al., 2008; MacGregor et al., 2009; 2016; Leysinger Vieli et al., 2011; Cavitte et al., 2018); or (c) integrating both their characteristics (e.g. elevation in the ice) and the information inferred from them (e.g. accumulation or basal--melt rates) to evaluate the output from regional and continental ice-sheet models (Leysinger Vieli et al., 2011; 2018; Holschuh et al., 2017; Sutter et al., 2021). Promisingly, Sutter et al. (2021) recently showed that spatially extensive Antarctic IRHs can provide unique benchmarks for constraining ice-sheet model parameterisations (i.e. climate forcing and simulated ice flow), which are then used to simulate palaeo ice-sheet evolution. Together, these studies indicate multiple avenues for ice-sheet models to assimilate IRHs further improve estimates of past, current and future ice-sheet changes.

Here, ~~our aim is to~~we estimate mid-Holocene accumulation rates across the WAIS from first-order calculations using a one-dimensional (1-D) model, ~~local-layer approximation (LLA) model (Waddington et al., 2007), informed~~ constrained by the spatially extensive 4.72 ka IRH. We first describe the data, the model used and their limitations and uncertainties~~We first describe the data and the 1-D model, and discuss the methods used to assess the feasibility of the LLA from gradients in horizontal ice-flow, ice thickness and accumulation-rate and how these translate into accumulation rate uncertainties~~ (Sect. 2). We then present our accumulation--rate estimates and ~~discuss~~ compare~~the effects of spatial and topographic controls on our results in relation~~ to observed and modelled modern accumulation rates ~~using both modelled gridded data from the Regional Atmospheric Climate Model~~

~~2 (hereafter RACMO2; Van Wessem et al., 2018) and observational point-based data from snow, firn and ice cores (Neumann et al., 2008; Burgener et al., 2013; Favier et al., 2013; Mayewski and Dixon, 2013; Medley et al., 2014),~~ to ~~generate~~ reveal a longer-term perspective on changes between the mid-Holocene and the present (Sect. 3). Finally, we place our results in the context of previous studies that consider WAIS ~~the~~ evolution ~~of the WAIS~~ during the Holocene (Sect. 4).

2. Data~~sets~~ and methods

2.1 Along-track IRH data

We used data from extensive (~91 000 flight-track km) RES surveys acquired across West Antarctica between 2004 and 2018. The main contributing surveys are the University of Texas Institute for Geophysics (UTIG) 2004-2005 AGASEA survey flown over Thwaites Glacier (THW) and Marie Byrd Land which deployed the 60-MHz High Capability Airborne Radar Sounder (HiCARS) radar system (Holt et al., 2006; Peters et al., 2007), and the British Antarctic Survey (BAS) 2004-05 BBAS survey over Pine Island Glacier (PIG) and 2010-2011 IMAFI survey over Institute and Möller Ice Streams (IMIS) which deployed the 150-MHz Polarimetric Airborne Survey INstument (PASIN) radar system (Vaughan et al., 2006; Corr et al., 2007; Ross et al., 2012; Fré~~e~~mand, Bodart et al., 2022) (Fig. 1; Table 1). Additional profiles from NASA's Operation Ice Bridge (OIB; MacGregor et al., 2021) 2016 and 2018 surveys, flown with the 190-MHz Multichannel Coherent Radar Depth Sounder 2 (MCoRDS-2) radar system (CReSIS, 2018), were also used to extract IRH information near the WD14 Ice Core and upper IMIS catchments (Bodart et al., 2021a; Figure 1 and Table 1). We refer the reader to the above references for comprehensive details on each system's capabilities.

189

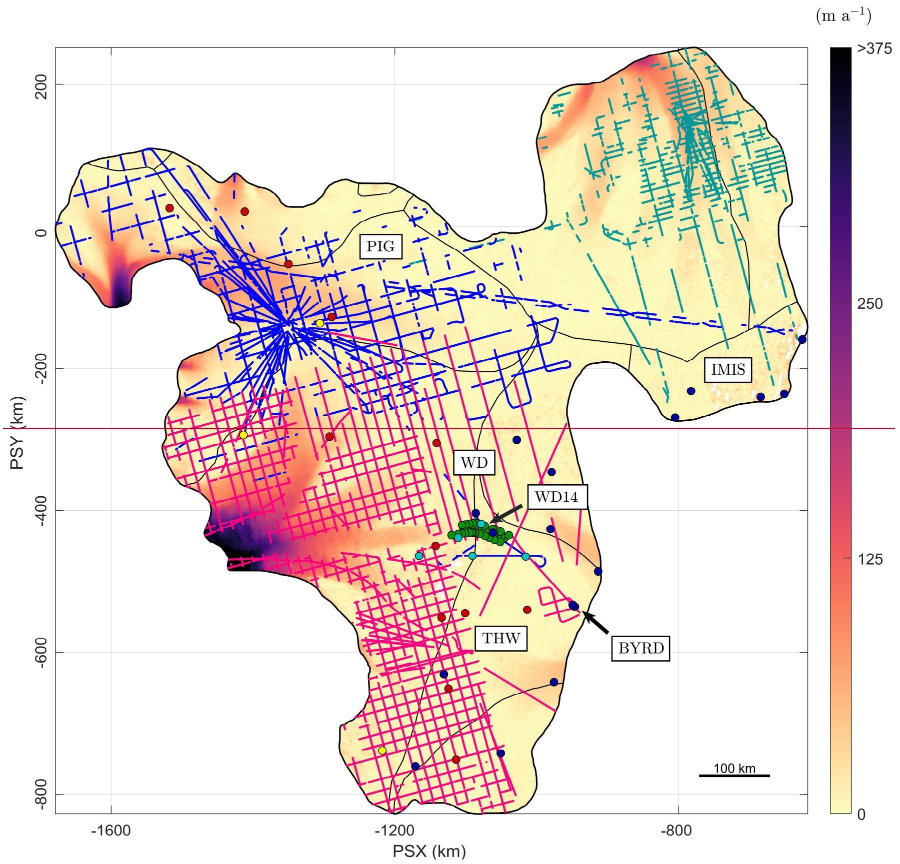
(m a⁻¹)
>375
250
125
0
200
0
-200
-400
-600
-800
PSY (km)
-1600
-1200
-800
PSX (km)
PIG
IMIS
WD
WD14
THW
BYRD
100 km

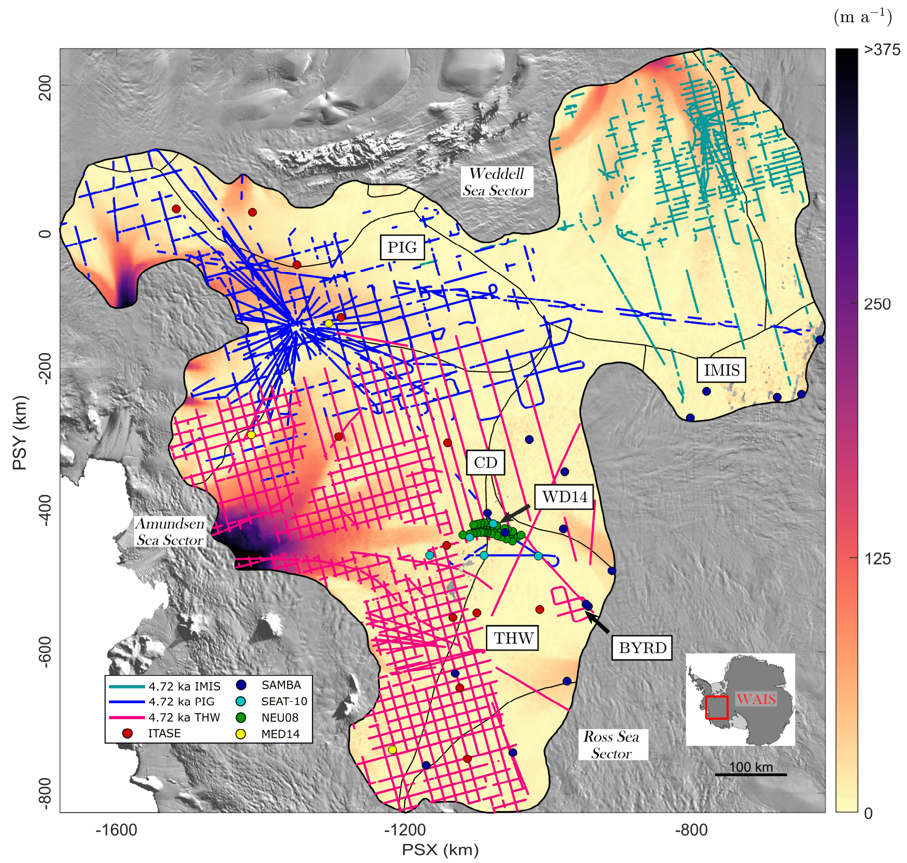

Figure 1. Map of the datasets and key locations in this study. The three datasets that contain the 4.72 ka IRH are colour-coded as IMIS (green), PIG (blue), and THW (pink). IRH ~~datas falling outside~~ where *D* >> 1 are excluded (see Section 2.2.1; Figure S1) ~~are excluded~~. Points ~~on the map~~ represent the snow, firn and ice cores used in this study to compare modern accumulation rates ~~of accumulation~~ with ~~our~~ those inferred from the 4.72 ka IRH ~~to-present estimates~~ (~~see~~ Sect.~~ion~~ 2.4 ~~for source references~~). The background colour map shows modern surface speeds from Rignot et al. (2017). Locations mentioned in this paper are abbreviated on the map, as follows: BYRD (Byrd Ice Core), IMIS (Institute and Möller Ice Streams), PIG (Pine Island Glacier), THW (Thwaites Glacier), WAIS (West Antarctic Ice Sheet), ~~WD~~ CD (Central Amundsen-Weddell-Ross Divide~~Western Divide~~), WD14 (WAIS Divide Ice Core). Major ice divides are from Mouginot et al. (2017). The background image is the 2014 MODIS mosaic of Antarctica (Haran et al., 2018). For all analysis and figures in this study, the ~~Projection for all figures in this paper is WGS84~~SCAR Antarctic Polar Stereographic projection is used (~~PSX/PSY;~~ EPSG: 3031).

These RES surveys were used to track and date six IRHs spanning ~~much of~~ the Late Pleistocene and Holocene ~~and Late Pleistocene~~ (25.7 – 2.3 ka BP) that collectively cover~~ing~~ much of the WAIS, ~~across~~ including IMIS (Ashmore et al., 2020a), PIG (Karlsson et al., 2014; Bodart et al., 2021a) and THW (Muldoon et al., 2018)~~, collectively spanning much of the WAIS~~. Here we only consider the 4.72 ka IRH mapped in all ~~three~~ four studies and shown in Figure 1, as it is by far both the most spatially extensive and the only commonly traced IRH across all studies. We first merged all data points from the 4.72 ka IRH across the three catchments, resulting in a cumulative distance of

~40 000 line-km of IRH profiles (44% of the RES surveys' total coverage; Table 1). Although the along-track RES data were acquired with a trace spacing of between 10 and 35 m, depending on the dataset used, we re-sampled these points to 500 m in the along-track direction. We then added a spatially invariant firn correction of 10 m onto the Muldoon et al. (2018) dataset to match the same firn correction applied by the other studies to correct the IRH depth.~~, and f~~ Finally, we calculated the median value of all ice thicknesses and IRH depths falling within ~~the nearest~~each 500 m interval.

Table 1. Characteristics of each IRH dataset used in this study that contain the 4.72 ka IRH. 'Reflector 1' in Muldoon et al. (2018) is abbreviated here as 'R1'.

Survey name	***Survey provider***	***RES system***	***Dataset reference***	***Cumulative IRH distance (10^3 km)***
IMAFI	BAS	PASIN 150-MHz	H2 in Ashmore et al. (2020a)	1~~.~~5~~x10^4~~
BBAS / OIB	BAS / NASA	PASIN 150-MHz / MCoRDS-2 190-MHz	R2 in Bodart et al. (2021a)	~~0.~~6~~x10^4~~
AGASEA	UTIG	HiCARS 60-MHz	R1 in Muldoon et al. (2018)	1~~.~~9~~ x10^4~~

2.2 Inferring accumulation rates

To infer accumulation rates from the 4.72 ka IRH, we used the Nye model, a 1-D ice-flow model widely used for estimating accumulation rates and age-depth relationships over relatively slow-flowing parts of an ice sheet (Nye, 1957; Fahnestock et al., 2001a). This model invokes the local-layer approximation (LLA), i.e. it assumes that the time-averaged accumulation rate that the IRH has experienced since its upstream inception at the surface can be adequately represented by its depth where it is observed presently. Other 1-D models exist, including the Dansgaard-Johnsen (Dansgaard and Johnsen, 1969) and the shallow-strain rate model (MacGregor et al., 2016), but ~~neither~~ were less suitable for estimating accumulation rates here ~~this study~~ due to uncertainty~~ies~~ in the basal shear layer thickness across our survey area and because we are limited to only one IRH to constrain the ice-flow model respectively. The Nye model assumes that ice thickness is constant and therefore that the ice sheet has been in a steady state since the deposition of the IRH, an ~~realistic~~ acceptable assumption for the period under investigation here. The Nye model states:

$$\dot{b}_a = \ln\left(\frac{z_a}{H}\frac{H}{a}\right), \tag{1}$$

where $\dot{b}_a$ is the mean ~~surface~~ accumulation rate during the Holocene epoch between an IRH of age a and the present, z_a represents the depth of the IRH dated at the ice core, and H is the ice thickness. The model assumes that the vertical strain rate, $\dot{\varepsilon}_a$, is also constant and vertically uniform, so that it exactly balances the overburden of local ice accumulation:

$$\dot{\varepsilon}_{zz}^{a} = \frac{\dot{b}_a}{H}. \tag{2}$$

We iterated Eq. (1) over the re-sampled 500-m spaced dataset using the depth of the 4.72 ka IRH for z_a and used the median radar-derived ice-thickness measurement re-sampled over the 500-m grid to obtain H, when this information was available. In areas where the radar did not sound the bed, we used the BedMachine Antarctic v2 gridded product to obtain a value for H (Morlighem, 2020). Note that ~~the~~ accumulation rate values presented in this study are all reported in m a^{-1} of ice equivalent.

~~Uncertainties in accumulation rates are calculated by iterating Eq. (1) using the lowest and highest possible age of the 4.72 IRH based on the maximum and minimum age uncertainty (± 0.28 ka) calculated from RES and ice-core depth uncertainties (see details in Muldoon et al. (2018) and Bodart et al. (2021a)). This results in lower and upper bounds in accumulation rates over our model domain (Fig. S2a-b), which are then combined to provide a relative uncertainty in accumulation rates for the 4.72 ka IRH (Fig. S2c). The maximum relative uncertainty in accumulation rates for the 4.72 ka IRH is 3.3%, with a median value of <0.5% across our grid. Note that these values do not include uncertainties due to the model approximation itself. As discussed in the next two sections, we believe model uncertainties to be small for the domain considered.~~

2.2.1 Assessing the suitability of the 1-D model

To quantify the suitability of the LLA ~~onto~~ from which ~~the~~ our accumulation rates~~1-D model is~~ are based, we calculated the effects of horizontal gradients in modern ice thickness and accumulation rates along particle paths in their ability to affect IRH depths across our grid, as per Waddington et al. (2007). ~~In places w~~Where these gradients are ~~too~~ large, estimates of accumulation rates from IRHs likely require a more complete treatment of ice flow ~~and strain rates~~ and its effect upon~~to account for disturbances in~~ IRH depths, which ~~only~~ multi-dimensional models and more physically complete models can better ~~are able to~~ resolve (e.g. Waddington et al., 2007; Leysinger Vieli et al., 2011; Karlsson et al., 2014; Nielsen et al., 2015; Koutnik et al., 2016~~; MacGregor et al., 2016~~). However, such models are significantly more computationally expensive over such a larger area and depend on well-constrained boundary conditions from along-flow radar profiles which are not often available at an ice-sheet level (MacGregor et al., 2009).

We quantified~~stimat~~ ~~To quantify~~ the effect of horizontal gradients on an IRH of age a by first estimating~~, we computed~~ the total horizontal particle path length L_{path} each “particle” of the 4.72 ka IRH has travelled since a, and then the characteristic lengths of variability in ice thickness (L_H) and apparent accumulation rate ($L_{\dot{b}}$)~~representing the gradients in ice thickness and accumulation rates respectively for age a~~ (Supplementary Information). These three components were then combined to generate a non-dimensional parameter D (Fig. S1d), which we used as a confidence metric for our inferred accumulation rates. Both Waddington et al. (2007) and MacGregor et al. (2009) suggested a value of $D \ll 1$ over Antarctica, whereas MacGregor et al.~~;~~ (2016) used a maximum value of $D = 1$ ~~value of unity~~ to estimate where the LLA is acceptable over Greenland. ~~but B~~Because ~~the value of~~ D cannot ~~yet~~ be translated simply~~quantitatively~~ into an uncertainty ~~value for~~ in an LLA-inferred accumulation rate, it is not yet clear what exact value is appropriate. Smaller values of D indicate that local horizontal gradients in ice thickness and accumulation rates have a smaller effect on IRH depth of age a, and thus ~~we can assume that~~ that the LLA ~~is~~ may be valid (Waddington et al., 2007; MacGregor et al., 2009; 2016). ~~However~~Where~~, if~~ $D \geq$~~>~~ 1, the depth of ~~the~~ an IRH is less likely to be ~~unlikely not necessarily~~ the result of ~~to be the sole result of~~ accumulation rates at the surface or vertical strain rates further down, and thus ~~that~~ a more sophisticated model is ~~thus~~ likely required (Sect. 2.2.2) (Waddington et al., 2007). However, MacGregor et al. (2009) found that even along a flowband across Lake Vostok where the mean value of D is 0.50 for a 41-ka IRH, the difference in accumulation rate inferred from the LLA and from a more sophisticated flowband model could be relatively small (4-16%). This similarly suggests that accumulation rate can be inferred acceptably using the LLA where D is higher.

~~In our case~~For our study area, ~~most of the survey areas has~~ D values are mostly ~~that are~~ well below ~~the~~ unity (median: 0.19; 25th quartile: 0.09; 75th quartile: 0.34), which suggests relatively little effect from ice-dynamical processes upon IRH depths across most of our grid. We used the upper quartile of the D distribution across our model domain (i.e. $D \leq 0.34$) to show areas where we can have confidence that accumulation rate remains the dominant factor influencing the vertical position of our IRHs in the ice column (i.e. where the $D \ll 1$ criterion is likely met; ~~see~~Fig. ~~Fig. 4,~~ S1d). While accumulation rates inferred from IRHs situated in the upper quartile (see Fig. S1d) may still be valid, we suggest additional caution in interpreting our results there due to the potential impact of larger flow gradients on IRH depths. a limited number of IRH profiles near the onset of PIG's tributaries and over THW's central trunk, which we excluded from our analysis.

2.2.2 Model limitations and uncertainty

One of the main limitations of the Nye model is that it assumes that gradients in sliding velocity are mostly concentrated in a thin layer at the ice-bed interface and that the ice column deforms by pure shear only (Nye, 1957; Fahnestock et al., 2001a). For this reason, the Nye model is generally only appropriate for IRHs found in the upper part of the ice column, as is the case here. Additionally, the use of the model is restricted to areas where ice flow is relatively slow and horizontal strain rates are also relatively low.

Here we focus on a shallower IRH situated in the upper part of the ice column (median: 40%; 25th quartile: 30%; 75th quartile: 50%; Fig. 2b-c), for which we can reasonably assume that the ice sheet has remained close to steady state and where IRHs are likely shallow enough not to have experienced appreciable flow disturbances that would affect the Nye model assumptions. Additionally, due to the inherent nature of tracking IRHs through RES data, our coverage is limited to areas where ice-flow speeds are relatively low and IRHs are undisturbed.

Whilst this is the case for most of our IRH coverage, In some portions of our study area, we note that some the IRH is found deeper in the ice column and/or in faster--flowing areassections of the ice sheet (e.g. in the downstream sectors of our grid, Fig. 1-2b-c); areas where the assumptions that the 1-D model is based on may be challenged.

Multi-dimensional models would likely improve the accumulation estimates for IRHs found in the lower half of the ice column or in more disrupted or faster flowing areas (e.g. Waddington et al., 2007; Neumann et al., 2008; MacGregor et al., 2009; Leysinger Vieli et al., 2011; Karlsson et al., 2014; Nielsen et al., 2015; Koutnik et al., 2016; Sutter et al, 2021); however, they are much more computationally expensive and depend on well-constrained boundary conditions from along-flow radar profiles which are not often available over such large regions (MacGregor et al., 2009).

HoweverHere, we focus on a shallower IRH situated within the upper 40%part of the ice column (median: 40%; 25th quartile: 30%; 75th quartile: 50%; Fig. 2b-c), where we can be reasonably confident that the ice sheet has remained close to steady-state and where IRHs are likely shallow enough not to have sustained appreciable disturbances that would affect the Nye model assumptions (Sect. 2.2.3).

Additionally, due to the inherent nature of tracking IRHs through RES data, our coverage is limited to areas where ice-flow speeds are relatively low and IRHs can be considered are relatively undisturbed. An assessment of strain rates over our model domain suggests limited disturbance over the WD and most of our grid, apart from near the onset of faster flow at the boundaries of our grid with the trunks of PIG and THW where higher strain rates are observed (Fig. S23). This pattern, combined with the assessment of the suitability of the LLA (Sect. 2.2.1) and exclusion of IRHs outside of the $D > 1$ boundary, supports our application of a 1-D modelling approach here.

Estimating uncertainty in accumulation rates from the Nye model is non-trivial. Previous studies have used the misfit between the accumulation rate calculated using multiple proximal IRHs in the ice column (e.g. Fahnestock et al., 2001a; 2001b; Leysinger Vieli et al., 2004; MacGregor et al., 2016). Unfortunately, this method is not suitable here due to the dearth of spatially extensive IRHs younger than 4.72 ka over our model domain.

Instead, uncertainty in the Nye-inferred accumulation rates were calculated using: (a) the lowest and highest possible accumulation rates from Eq. (1) using the age uncertainty (± 0.28 ka) of the 4.72 ka IRH and (b) the lowest and highest possible accumulation rates inferred from an additional 1-D model (Eq. S5) which accounts for the effect of strain rates on accumulation rates (i.e. the shallow-strain rate model from MacGregor et al. (2016); Supplementary Information; Fig. S2-4).

This calculation provides lower and upper bounds for the IRH-inferred accumulation rates (Fig. S4a-b), which were then averaged to generate a relative uncertainty (Fig. S4c). From this assessment, we estimate a median relative uncertainty in the Nye-inferred accumulation rates for the 4.72 ka IRH of 14% across our grid. This uncertainty is higher in the downstream edges of our grids, particularly over the PIG, THW and IMIS catchments, and generally low over the Amundsen-Weddell-Ross divide (Fig. S4), reflecting the effect of spatially variable strain rates on the inferred accumulation rates. When combined with the assessment of the suitability of the LLA and exclusion of IRHs where the $D > 1$ (Sect. 2.2.1-2.2.2), we conclude that it supports our application of a 1-D modelling approach here.

2.3 Gridding and filtering

Once IRH depths and accumulation rates for the 4.72 ka IRH were obtained at regular 500-m points along RES flight paths, we filtered the results using a moving-average Gaussian filter of length 30 samples (equivalent to ~15 km) to reduce along-track noise in the IRH depth, and then gridded the filtered result using a Delaunay-triangulation-based natural neighbour interpolation method onto a 1-km polar stereographic grid. We further smoothed the gridded data using an 18-km square cell mean filter to limit the localised interpolation artefacts~~ arising from the interpolation, which can be problematic~~ in areas ~~with~~ of poor ~~data~~ survey coverage. Figure S5~~4~~ shows the maximum distance away from the nearest 500-m along-track point used to produce Figures 2-3, and thus where errors in the interpolated grids are expected to be larger. The median value of this maximum distance is 5 km and its maximum value is 75 km, which is comparable to previous studies that infer ~~Surface Mass Balance (SMB)~~ SMB from IRHs in the shallow firn (e.g. Medley et al., 2014). We evaluated other possible interpolation methods (e.g.~~,~~ kriging and using different semi-variogram models), but they resulted in similar or poorer quality~~,~~ and were thus discounted.

2.4 Comparison with modern observations

To compare our inferred accumulation estimates for the past 4.72 ka with modern values ~~times~~ (defined here as 1651-2019), we derived information on modern accumulation rates from two sources, one modelled (gridded) and one from a series of observational (point-based) datasets.

We used modelled gridded accumulation rates from the Regional Atmospheric Climate Model 2.3p2 (hereafter RACMO2) ~~RACMO 2.3p2~~ 1979-2019 ~~Surface Mass Balance (~~SMB~~)~~ product forced at its margin with the ERA-Interim product (native resolution: 27 km) as an estimate for modern accumulation rates (Van Wessem et al., 2018). Although SMB is not technically equivalent to the accumulation rate, runoff and sublimation are negligible in our survey area (Medley et al., 2013) so we ~~consider~~ assume SMB is equal to accumulation rate in this region. We converted modelled values from kg m^{-2} a^{-1} to m a^{-1} of ice equivalent using an ice density value of 917 kg m^{-3}, calculated the 40-year mean, and then bi-linearly interpolated the gridded RACMO2 product to the same 1-km grid resolution as our 4.72 ka-to-present accumulation grid (Sect. 2.3) to ensure consistency when comparing both datasets.

Observational point-based measurements were obtained from a series of snow, firn and ice cores from the ITASE (Mayewski and Dixon, 2013), MED14 (Medley et al., 2014), SAMBA (Favier et al., 2013), and SEAT-10 (Burgener et al., 2013) datasets, as well as from a network of centennially-averaged modern accumulation rates derived from shallow IRHs traced on ground-based RES data over the central divide ~~WD~~ and dated using a shallow ITASE Ice Core (Neumann et al., 2008) (Fig.

1). This ~~results~~ resulted in 79 point-based accumulation measurements from cores covering the period 1651-2010 CE (Common Era) and spread across our model domain (see Figure 1). Further detail on these datasets can be found in the above references.

To compare the Holocene gridded product with the point-based measurements, we first calculated the average value of the accumulation rate at the point measurement for the entire period. We converted these~~is~~ values to ice-equivalent accumulation rates ~~(as above)~~ and then extracted ~~the~~ two paired values, i.e.~~,~~ the value for the point-measurement for modern accumulation rates and the value for the nearest grid cell in the gridded 4.72 ka-to-present accumulation estimates to this measurement.

3. Results

The final grids for depth and accumulation rates for the 4.72 ka IRH are shown in Figures 2 and ~~–~~ 3. In total, these grids are made of ~89 000, 500-m spaced points, which cover an area of ~610 000 km^2, or ~30% of the total surface area of the WAIS. The grids span most of the PIG and THW glacier catchments, as well as the Ronne (upper Rutford, Institute, and Möller) and upper western Ross (Bindschadler, Kamb, MacAyeal, and Whillans) catchments (IPY Antarctic boundaries G-H, J-Jpp, and Ep-F; Mouginot et al. (2017); Fig. 1-2). Overall, the 4.72 ka IRH is shallower within the IMIS and upper PIG and THW catchments, as well as on the Ross side of the ~~WD~~ central divide where ice thickness is particularly deep (Fig. 2b). Conversely, the 4.72 ka IRH is deeper in the ice near a 400-m high bedrock plateau that separates the northern and southern basins of PIG (Vaughan et al., 2006) and at two locations in the upstream parts of the main trunk of THW where ice flows over highs in subglacial topography (Fig. 2b).

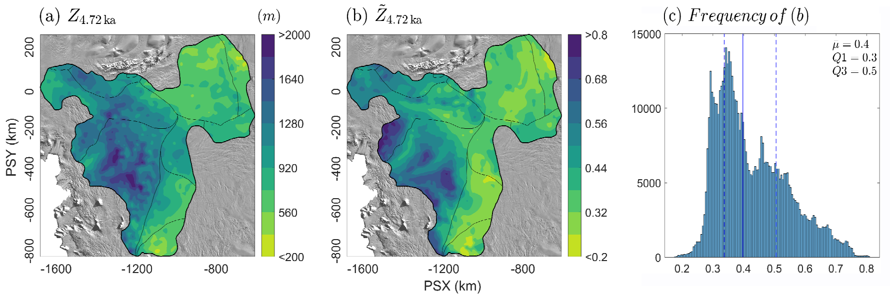

Figure 2. Gridded depths for the 4.72 ka IRH across the model domain covering the PIG, THW, and Institute and Möller ice-stream catchments. (a) Gridded depth of the 4.72 ka IRH. (b) Normalised depth of the 4.72 ka IRH relative to ice thickness. (c) Histogram showing the distribution of values in (b) with the median ($\tilde{\mu}$) and ~~the~~ interquartile range (i.e. 25th (Q1) and 75th (Q3) quartiles) shown as solid and dashed blue lines respectively. The background image is the 2014 MODIS mosaic of Antarctica (Haran et al., 2018).

3.1. Catchment-scale accumulation estimates

Figure 3 shows a comparison of the ice-equivalent accumulation rates we inferred for the 4.72 ka IRH (Fig. 3a) and modern SMB estimates from RACMO2 (Fig. 3b). We observe that the IRH accumulation rate pattern for the last 4.72 ka is similar to the modern pattern of accumulation rates for the Amundsen Sea sector of the WAIS, which is dominated by higher coastal accumulation rates that progressively decrease inland ~~towards the ice divides~~to reach their lowest rates over the Ross side of the divide (Fig. 3a-b). Differences in accumulation rates between the 4.72 ka-to-present estimates and modern values are mainly observed directly upstream of the main trunks of PIG and THW, where modern rates are much higher (up to 0.2 m a^{-1} ice equivalent) than for the 4.72 ka-to-present estimates (Fig. 3c). In comparison, higher accumulation rates for the last 4.72 ka ~~compared~~ relative to modern rates are observed for the entire stretch of the Amundsen-Weddell-Ross divide~~WD~~ (Fig. 3c; Table 2). ~~Noticeably over~~Over the IMIS catchment, little change is observed between the two periods. Over the entire model domain, we observe a median ~~relative increase~~percentage change value of ~~13~~6% ~~in~~ higher accumulation ~~rates~~ since 4.72 ka compared with modern rates (Fig. 4~~; Table 2~~); however, when considering only the values that fall within 100 km of either side of the Amundsen-Weddell-Ross divide~~WD~~ (i.e. in the accumulation zone of the Amundsen, Weddell, and Ross Sea sectors and where mean surface speeds ~~equal~~ average ~7 m a^{-1}), we obtain a median percentage change value of 18% higher accumulation compared with modern accumulation rates (Fig. 4).

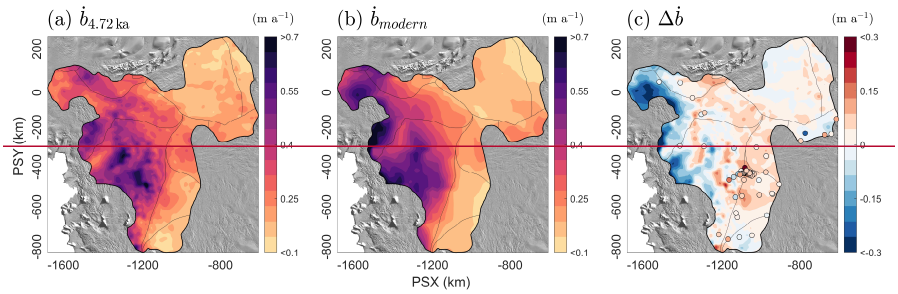

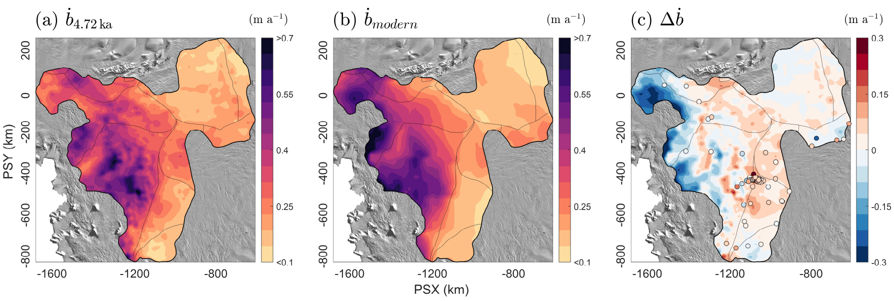

Figure 3. Gridded estimates of ice-equivalent accumulation rates for the last 4.72 ka and modern times. (a) Gridded accumulation rates inferred from the 4.72 ka IRH. (b) Modern (1979 – 2019) modelled SMB rates from RACMO2. (c) Difference between 4.72 ka-to-present and modern accumulation rates (red = 4.72 ka-to-present accumulation higher than modern times, blue = 4.72 ka-to-present accumulation lower than modern times). The dots represent the difference between the value for the nearest grid cell in (a) and time-averaged accumulation rates at each of the 79 core locations (see Section 2.4; Fig. S6). The background image is the 2014 MODIS mosaic of Antarctica (Haran et al., 2018).

Comparison between our 4.72 ka-to-present accumulation-rate estimates and 79 core-derived point-based accumulation measurements for modern times (1651-2010 CE) are shown in Figures ~~3 and 3-~~4 and S6. This evaluation shows that the 4.72 ka-to-present accumulation-rate estimates for the nearest grid cell to each point measurement are, on average, ~~18~~22% ~~(p < 0.0015, n=79)~~ higher for cores situated ~~over~~ across the entire grid (p < .0015, n=79) and ~~19~~23% ~~(p < 0.0001, n=59)~~ higher for cores found within 100 km of the divide ~~than~~ compared with modern accumulation rates (p < .0001, n=59; ~~(~~Figs. 4 and S6). In comparison, a similar analysis between grid cells from the 4.72 ka-to-present accumulation-rate estimates and RACMO2 at these 79 core locations shows mid-Holocene accumulation rate estimates are, on average, 32% (P < .00002, n=79) higher for cores situated across~~over~~ the entire grid and 36% higher for cores found within 100 km of the divide (p < .00001, n=59; Fig. S6). This result confirms that the relative ~~difference~~ change ~~in~~for gridded accumulation rates between the 4.72 ka-to-present and modern modelled accumulation rates is consistent with modern rates from point-based measurements.

Table 2. Summary statistics for the modern (modelled and observational) and 4.72 ka-to-present ice-equivalent accumulation rates at the catchment-scale and over the Amundsen-Weddell-Ross divide~~WD~~. Values for the Amundsen-Weddell-Ross divide (abbreviated CD here)~~WD~~ are for all points that fall within 100 km of either side of the divide (see dashed line in Figure 4). $\tilde{\mu}$ refers to the median and IQR represents the Interquartile Range calculated by computing the difference between the 75th and 25th percentiles. Note that the values provided in the text represent the median relative change from the cell-by-cell change between each grid (Fig. 4), rather than the relative change of the median values provided here.

	Catchment-wide		***~~WD~~ CD only***	
Accumulation rate (m a^{-1})	$\tilde{\mu}$	***IQR***	$\tilde{\mu}$	***IQR***
Modern (model)	0.23	0.23	0.22	0.10
Modern (cores)	0.24	0.12	0.24	0.09
4.72 ka-to-present	0.27	0.18	0.27	0.11

~~For WD14 specifically, the nearest grid node to the ice-core site shows a 22% higher accumulation rate from 4.72 ka to present compared with modern accumulation rates (Fig. 4). There, our IRH-inferred accumulation rate is 0.28 ± 0.01 m a^{-1}, with the nearest IRH point situated 1.2 km away from WD14 showing an accumulation rate of 0.27 ± 0.01 m a^{-1}. This is only slightly higher than the direct ice-core reconstruction of accumulation rates at WD14, which show up to 19% (0.25 m a^{-1}) higher accumulation than modern rates (0.21 m a^{-1}) since 4700 years BP (Fudge et al., 2017).~~

464 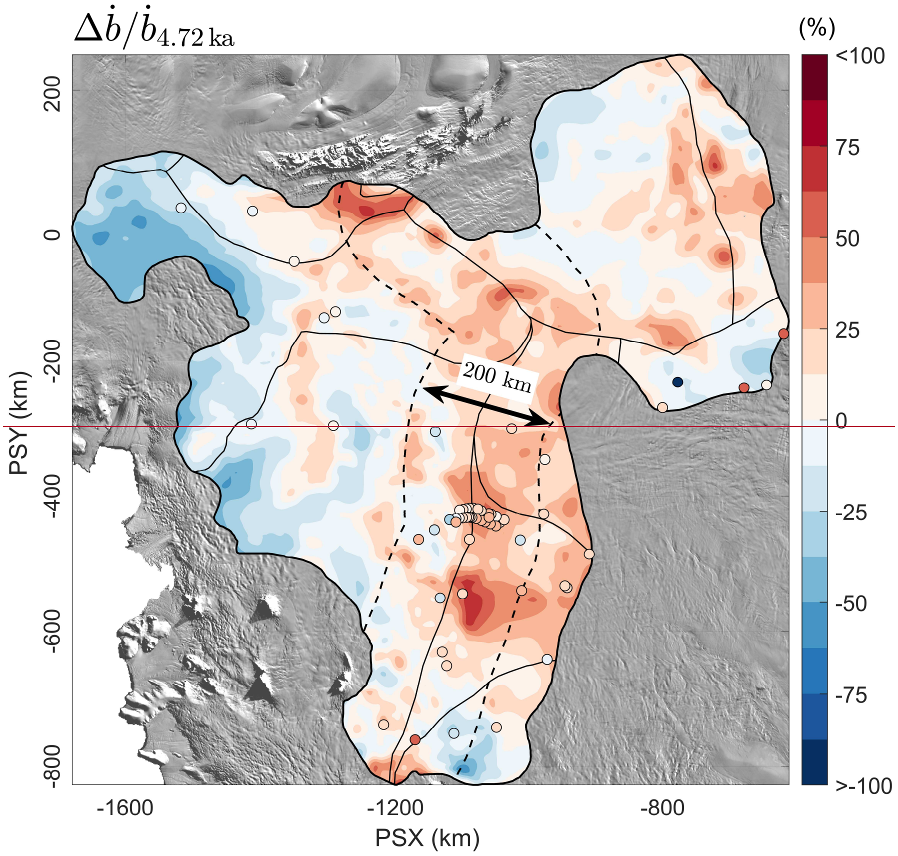
$\Delta\dot{b}/\dot{b}_{4.72\,\mathrm{ka}}$
(%)
<100
75
50
25
0
-25
-50
-75
>-100
200 km
PSY (km)
200
0
-200
-400
-600
-800
-1600
-1200
-800
PSX (km)

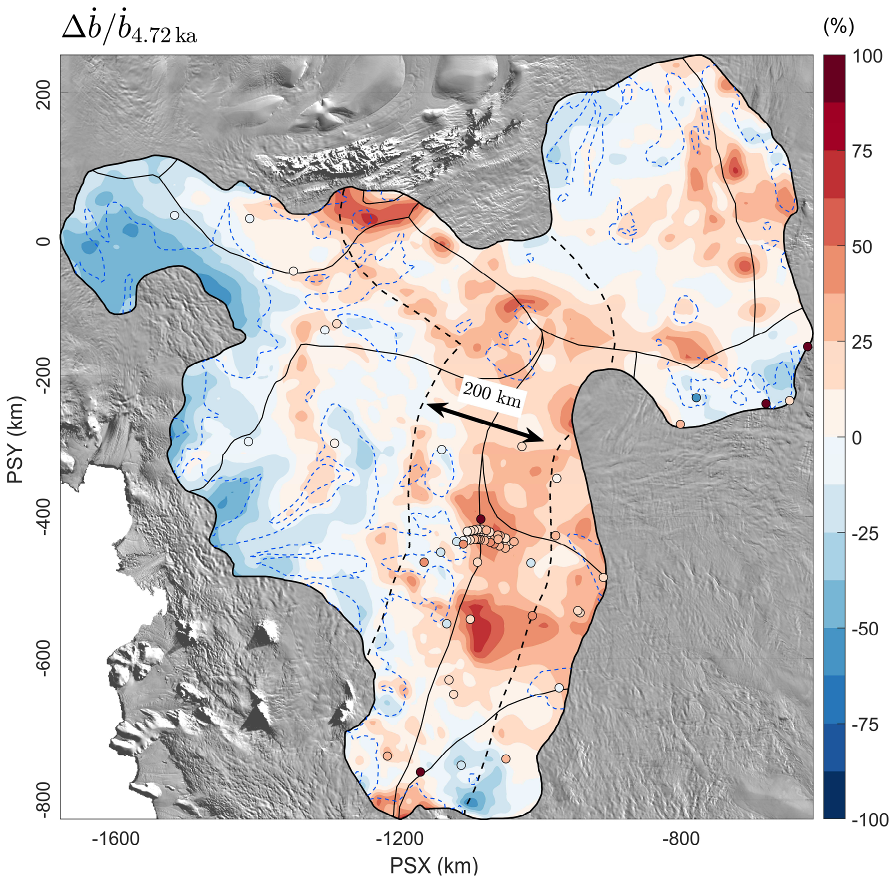

Figure 4. Relative ~~difference~~ change in accumulation rates between the 4.72 ka-to-present estimates and modern rates. The points on the map represent the relative ~~difference~~ change in ice-equivalent accumulation rate between the nearest grid cell in the 4.72 ka-to-present grid and the 79 modern observations from cores ~~al accumulation measurements from snow, firn, and ice cores~~ (Figs. 1 and S65; ~~see~~ Sect. 2.4). The dashed black outline line represents the 100-km boundary on either side of the Amundsen-Weddell-Ross divide~~WD~~ used to provide the summary statistics in Section 3.1 and Table 2. The dashed blue line shows the contours of the upper limit of the interquartile range for the *D* parameter ($D \leq 0.34$) (Sect. 2.2.1-2.2.2). The background image is the 2014 MODIS mosaic of Antarctica (Haran et al., 2018).

3.2 Elevation-dependent accumulation estimates

While Figures 3 and 4 help to assess potential differences in patterns and rates across spatial scales, considering accumulation-rate differences in terms of elevation can inform how topography influences accumulation and whether this has changed over time. ~~As a resultw~~We binned the ice-equivalent accumulation values ~~for each~~by 50-m elevation bands across the ~~our model domain~~ three main catchments covering our grid (Amundsen, Weddell and Ross) for both the 4.72 ka-to-present estimates and modern model rates ~~(RACMO2),~~ and calculated the mean accumulation rate and~~,~~ the total accumulation rate ~~, and the cumulative sum of total accumulation rate~~ for each bin over the entire elevation gradient ~~of the two grids~~ (Fig. 5). ~~As above, w~~We again find ~~observe~~ that the accumulation-rate estimates for the period since 4.72 ka are lower at low~~er~~ elevations (~700 – 1400 m) over the Amundsen sector compared with RACMO2, ~~and~~ but begin to exceed ~~overtake~~ RACMO2 near the 1400-m elevation band where the 4.72 ka-to-present accumulation rate is higher than modern times across the divide ~~up until ~24600 m in elevation~~ (Fig. 5a-b). We also note that whilst an elevation-dependent gradient in accumulation rates, dominated by high accumulation at the coast decreasing inland, exists over this sector for the mid-Holocene, it is much less marked than for present rates. This is not surprising, as this sector is where we observe the largest relative uncertainties in inferred accumulation rates across our grid (Fig. S4), indicating that the 1-D model is less able to produce realistic accumulation rates in the downstream end of our grid where ice flow is faster and strain rates are likely higher. In comparison to the Amundsen sector, accumulation rates since 4.72 ka are generally higher at all elevations for the Weddell and Ross sectors compared with the present, although this difference is less than over the Amundsen sector (Fig. 5 c-f). ~~The lack of a large difference between the two datasets at elevations of ~250 – 700 m is primarily dominated by accumulation rates over IMIS, which, in contrast to the PIG and THW regions, is less exposed to the large accumulation gradients characteristic of the Amundsen Sea Embayment, i.e. higher coastal accumulation decreasing inland.~~

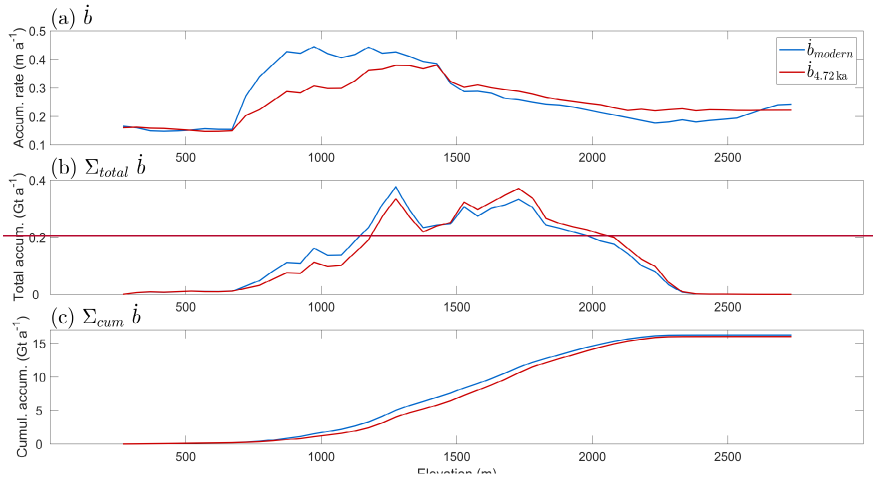

Formatted: Indent: First line: 0.63 cm

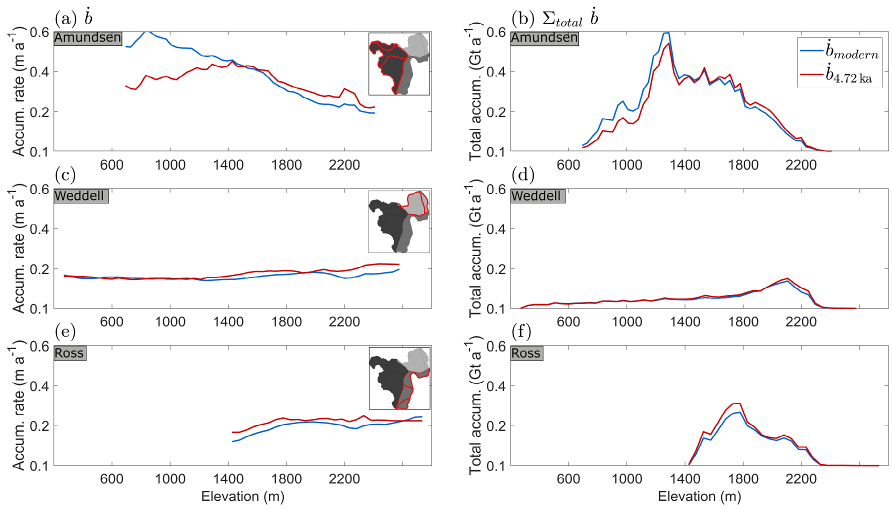

Figure 5. Comparison of ice-equivalent accumulation rates between the 4.72 ka-to-present estimates and modern rates (RACMO2) binned ~~for each~~by 50-m elevation bands across ~~our study~~the three main catchments considered here (Amundsen, Weddell, and Ross). (a, c, e) Mean accumulation rate averaged per 50-m elevation band across the ~~survey~~ specific catchment area in m a^{-1}~~Fb~~. (b, d, f) Total accumulation rate per 50-m elevation band across the specific catchment area in Gigatonnes ~~Gigatons~~ per annum (Gt a^{-1}). ~~(c) Cumulative sum of total accumulation rate per 50-m elevation band in Gt a^{-1}.~~

4. Discussion

4.1. Comparison with other Holocene accumulation estimates

Formatted: Indent: First line: 1.27 cm

Previous studies of past accumulation rates over the WAIS have shown that accumulation varied temporally during the Holocene. Using a single airborne RES profile over the Amundsen Sea sector, Siegert and Payne (2004) showed that accumulation rates were approximately the same at 3.1 ka compared with modern rates, but ~0.3 m a^{-1} greater (~15 %) than current rates between 3.1-6.4 ka, before which accumulation was ~50% of modern rates between 6.4 and 16.0 ka. Similarly, Neumann et al. (2008) found that accumulation rates at the ~~WD~~ central divide were ~30% higher between 3-5 ka than modern values based on a dense network of IRHs traced on ground-based RES data, while Karlsson et al. (2014) found that accumulation patterns had likely changed twice during the early to mid-Holocene over PIG from the lack of a model fit between the depths and ages of two prominent IRHs. Using the updated WD14 record, Fudge et al. (2016) showed that accumulation rates ~~was~~ were higher there in the mid to late-Holocene (19% between 4.72 ka BP and the present), a trend that was also observed by Koutnik et al. (2016), who found a 20% increase in accumulation rates between 2-4 ka compared with modern rates from a ground-based RES profile across the ice divide.

These studies together point to a period of increasing accumulation observed at the WD14 Ice Core from ~7 ka onwards (Fudge et al., 2016; their Figure 2), with its peak matching the age of the 4.72 ka IRH used here. Thus, our accumulation-rate estimates likely form part of a wider pattern of a sustained increase in accumulation across the Amundsen-Weddell-Ross divide~~WD~~ over several millennia. In showing that mean accumulation rates since 4.72 ka were 18% greater than modern rates modelled from RACMO2 across the Amundsen-Weddell-Ross divide~~WD~~, our results provide ~~a~~ much wider regional ~~picture~~ support for the hypothesis~~(across ~30 % of the WAIS)~~ that accumulation rates during the mid-Holocene exceeded modern rates ~~over~~ across ~~large parts of~~central West Antarctica.

~~We gain confidence in the ability of the Nye model to estimate past accumulation rates from the 4.72 ka IRH, given that its outputs match relatively well with the direct reconstruction of mean accumulation rates at the WD14 Ice Core, with values at the ice core of 0.27 ± 0.01 m a^{-1} (this study) compared with 0.25 m a^{-1} for Fudge et al. (2016). This also suggests that the WD14 Ice Core suitably represents atmospheric conditions across the wider WD.~~ A possible explanation for ~~the higher accumulation rates~~this pattern ~~during the mid-Holocene compared with modern values~~ is that they represent a continued climatic transition from the LGM (Steig et al., 2001). Alternatively, it has been suggested that seasonal or interannual variability, such as a weaker circumpolar vortex (v~~V~~an Den Broeke and ~~V~~van Lipzig, 2004; Neumann et al., 2008), or teleconnections to tropical Pacific Ocean warming (Sproson et al., 2022), may also lead to such difference. We did not find evidence for significant changes in accumulation patterns between the mid-Holocene and modern times, suggesting that the current spatial pattern of high accumulation ~~at the~~on the Amundsen side of the divide ~~coast~~ transitioning to~~, decreasing~~ low accumulation ~~inland towards at the divide~~on the Ross side of the divide was stable throughout the mid-Holocene ~~over PIG and THW~~, as previously suggested by others (Siegert and Payne, 2004; Neumann et al., 2008; Koutnik et al., 2016).

We also find that a~~A~~ccumulation estimates for the 4.72 ka-to-present are smaller than modern rates in the lowest elevation bands (~~i.e.~~ <1400 m), particularly over~~, particularly over~~ the Amundsen Sector (Fig~~s~~. ~~4, ~~5 a-d). This pattern was also ~~reported~~ found by Medley et al. (2014), who compared modern observational and modelled data ~~within~~ over th~~e ASE~~is sector and hypothesised that this discrepancy at low elevations resulted primarily from a lack of sufficient accumulation measurements in the lower sections of their survey area. In our case, these low-elevation values are close to the boundary where we consider the LLA acceptable for the 4.72 ka IRH, albeit where *D* values are higher than for the rest of the catchment (Figure S1d), so it is more likely that accumulation rates calculated there are affected by ice-flow gradients and their influence upon IRH depths leading to lower accumulation rates there. Despite this caveat, Figures 5b and 5d show~~s~~ that values at low elevations ~~(250 – 1200 m)~~ contribute relatively little to the total accumulation (by mass) over our survey area.

We suggest that future ice-sheet modelling studies investigate the difference in accumulation rates inferred from our 1-D model using multi-dimensional flowband models to assess effects of divergent and convergent flow on IRH depth and ultimately accumulation rates, as previously considered elsewhere in Antarctica (MacGregor et al., 2009). This could be conducted along a flowline transitioning from the slow-flowing regions directly downstream of the Amundsen-Weddell-Ross divide~~WD~~ to the coastal margins of our grid, particularly over THW where we observe the largest uncertainties in accumulation rates. In addition, we suggest that future modelling studies use the accumulation-rate variability from the WD14 Ice Core as a climate forcing in their ice-sheet models. Koutnik et al. (2016) previously showed that the WD14 record is unique in that it provides a reliable record of accumulation-rate variability during the Holocene, which other East Antarctic ice-core records often used to reconstruct the evolution of the WAIS do not possess. We found that these higher accumulation rates are spatially extensive across nearly one third of the WAIS, further suggesting that the WD14 Ice Core is indeed representative of the wider WAIS and can be used in regional or continental ice-sheet models as a reliable climate forcing for the region. Future regional and continental ice-sheet models should make use of this record to adjust their climatic boundary conditions to provide improved estimates of ice-elevation change and grounding-line evolution over Antarctica.

4.2 Impact for ice-sheet elevation change during the Holocene

Formatted: Indent: First line: 1.27 cm

~~Our results reinforce the evidence that accumulation rates have varied temporally across West Antarctica during the Holocene, a finding that must be considered by future modelling studies that simulate past sea-level rise from Antarctica since the LGM.~~ Model results from Steig et al. (2001)

suggest that the maximum elevation of the WAIS was most likely reached during the early to mid-Holocene (around ~7 ka) following higher accumulation rates at the late glacial–interglacial transition, after which ~~elevations~~ the WAIS slowly declined to present conditions as the sea-level-rise-induced kinematic wave reached the ice-sheet interior and outpaced the increase in accumulation rates. However, ~~a moderate mid-Holocene increase in accumulation rates~~higher accumulation rates in the mid-Holocene relative to the present, which our results suggest occurred ~~widely~~ spatially across the WAIS, would~~, if sustained,~~ likely delay the timing of th~~e~~is thinning ~~decline in elevation~~ by several thousand years (Steig et al., 2011).

Using a flowband model, Koutnik et al. (2016) suggested that ~~the~~ an increase of up to 40% in accumulation rates for the period 9 – 2 ka would likely have le~~a~~d to an increase in ice thickness of tens of metres~~ers~~ during the mid-Holocene. Although this finding was warranted by physical assumptions around the response time of the ice-sheet interior to adjust to an increase in accumulation in the model, it points to the potential for the divide to have thickened by several metres over a relatively short period of time from increased accumulation rates alone. ~~HoweverThis noted, because~~ Because the WAIS is also sensitive to ice-dynamical changes at the ice-sheet margins (e.g. grounding-line~~GL~~ retreat ~~and~~/or calving), an increase in accumulation rates in the upper part of the ice sheet may not necessarily result in enough thickening to counteract potential dynamical losses ~~from ice dynamics~~ fa~~u~~rther downstream (Jones et al., 2022). Conway and Rasmussen (2008) reported that the ~~WD~~Amundsen-Ross Divide is currently thinning and migrating towards the Ross Sea at a speed of 10 m a^{-1}, but they were unable to determine whether this was in response to long-term (last two millennia) accumulation-rate changes there or short-term (last few centuries) ice-dynamical forcing from the coastal margins of the Amundsen and Ross sectors. More recently, Balco et al. (2023) showed that Thwaites and Pope glaciers experienced 35 m of thickening in the mid-to-late Holocene, when accumulation rates were higher than present. While this thickening relative to present was attributed to glacio-isostatic rebound, it is also possible that higher accumulation rates in the upstream sections of the WAIS contributed to this thickening, if sustained over millennia.

The lack of an ice-dynamical component in the model used here precludes us from ~~reaching~~ evaluating any ice-surface-elevation change associated with changing~~such a conclusion; however, higher~~ accumulation rates. However, ~~of up to~~ ~~at least~~ 18% higher accumulation rates during the mid-Holocene relative to the present across 30% of the WAIS c~~w~~ould ~~likely~~ be consistent with an elevation increase of several tens of metres~~ers~~ in ice thickness, according to Koutnik et al. (2016) ~~(e.g. Figure 10 of Koutnik et al., 2016)~~. Even if tens of metres of ice-surface-elevation change occurred, it ~~This potential increase in surface elevation~~ is still unlikely to significantly affect the steady-state assumption of the 1-D model used here (constant ice thickness over time), because such~~considering that these~~ changes are small (a few per cent of the ice thickness) and that ice thickness exceeds 3500 m in places over our survey area.

Formatted: Indent: First line: 1.27 cm

~~We encourage future ice-sheet models to test a range of scenarios that would account for variable accumulation rates between the LGM and the present over the WAIS by using the WD14 reconstructed accumulation rates from Fudge et al. (2016) as a guide, which, as we show here, suitably represents the pattern of accumulation variability over both time and space in West Antarctica.~~

4.3 Impact for grounding-line evolution during the Holocene over the WAIS

Formatted: Indent: First line: 1.27 cm

Finally, w~~W~~e ~~may also~~ consider the possibility for Holocene ice thickening at the divide from increased accumulation rates to affect downstream grounding-line~~GL~~ evolution ~~over the WAIS~~. Recent evidence from ice-sheet modelling and field measurements suggest~~s~~ that grounding-line~~GL~~ retreat during the Holocene was not monotonic, particularly at the Ross and Weddell Sea sides of the WAIS (Bradley et al., 2015; Kingslake et al., 2018; Neuhaus et al., 2021). Rather, Kingslake et al. (2018) showed that the grounding-line~~GL~~ position in the Ross and Weddell Sea sectors initially retreated from the LGM inland until ~10.2 – 9.7 ~~9.7 – 10.2~~ ka, and then re~~-~~advanced to its modern position sometime during the Holocene. Although they attributed this change in grounding-line~~GL~~ position to the solid Earth viscoelastic response due to ice-sheet mass change and the subsequent re-grounding around pinning points, it has also been suggested that an increase in accumulation rates upstream of the grounding line~~GL~~ could lead to a re~~-~~advance via ice thickening there and a subsequent increase in ice flow (Steig et al., 2001; Koutnik et al., 2016; Jones et al., 2022). Across parts of the Weddell Sea Embayment, several studies ~~(Ross et al., 2011; Hein et al., 2016; Ashmore et al., 2020a)~~ have produced evidence for stability of the LGM ice thickness there until the early to mid-Holocene (Ross et al., 2011; Hein et al., 2016; Ashmore et al., 2020a), contrary to most of the WAIS, after which abrupt thinning of ~400 m contributed ~1.4 – 2 m of sea level rise (Hein et al., 2016). A possible explanation for this delayed thinning in the Weddell Sea Embayment is that increased snowfall in the upper WAIS might have counteracted ice-dynamical processes at the coast until the mid-to-late Holocene (Hein et al., 2016; Spector et al., 2019). Similarly, over part of the Ross Sea sector, Neuhaus et al. (2021) showed that the grounding line~~GL~~ over Whillans, Kamb, and Bindschadler ice streams retreated to its minimum Holocene position in the mid to late-Holocene, and then re~~-~~advanced between 2 – 1 ~~1 – 2~~ ka, coinciding with periods of warmer and colder climates, respectively. They concluded that the reported grounding-line~~GL~~ migration was likely dominated by modest climate-induced changes upstream rather than ice dynamics further downstream, as suggested for the Weddell Sea sector (Hein et al., 2016).

Our results, which provide strong and widespread evidence for higher accumulation along the Amundsen-Weddell-Ross divide during the mid-Holocene compared with the present, support these hypotheses further, as higher accumulation rates at the divide would likely result in upstream thickening (Sect. 4.2). In the absence of ice-dynamical processes counter-balancing this increase in accumulation rates, the grounding-line should advance in these regions. However, we note that the pattern of grounding-line retreat and readvance has not been observed over the Amundsen Sea sector (Kingslake et al., 2018; Johnson et al., 2020; 2021; Braddock et al., 2022) despite the accumulation-rate increase we also observed along the Amundsen-Weddell-Ross divide and the recent results from Balco et al. (2023). This complication may indicate that the Amundsen sector is more strongly influenced by coastal changes in ice dynamics, for which even moderate changes in accumulation rate cannot compensate.

5. Conclusion

Formatted: List Paragraph, Numbered + Level: 1 + Numbering Style: 1, 2, 3, … + Start at: 1 + Alignment: Left + Aligned at: 0.63 cm + Indent at: 1.27 cm

Using a ubiquitous i~~I~~nternal r~~R~~eflecting h~~H~~orizon found across most of the Pine Island, Thwaites, and Institute and Möller ice-stream catchments, we have estimated mid-Holocene accumulation rates in the relatively slow-flowing parts of West Antarctica, ~~(~~representing 30% of total surface area of the WAIS~~) using a 1-D ice-flow model~~.

By comparing our Holocene accumulation-rate estimates with a modern climate reanalysis model~~s~~ and observational syntheses, we estimated that accumulation rates across the Amundsen-Weddell-Ross Sea divide since 4.72 ka were, on average, 18% higher than modern ~~accumulation rates~~values. ~~While the accumulation rates have therefore varied temporally, o~~Our results suggest that spatial patterns of accumulation ~~between regions across the~~across the WAIS have remained ~~similar~~ stable during this period, i.e.~~,~~ higher accumulation rates on the Amundsen side of the divide ~~at the coast and~~ transitioning to lower accumulation rates ~~at the ice~~on the Ross side of the divide~~s~~. The higher accumulation rates ~~estimates~~ reported here for the mid-Holocene compared to the present agree well with ~~previous~~earlier, ~~more~~ spatially-focused studies of accumulation rates ~~across the WAIS~~, all of which ~~which all~~ indicate higher accumulation rates ~~of between~~ (+15 ~~and~~ - 30%) over the p~~l~~ast ~5 ka ~~compared with the present~~. This change in magnitude occurred at a time of asynchronous grounding-line migration over the WAIS, including re-advances of the grounding line in the Weddell and Ross sectors and evidence for delayed deglaciation in the Weddell Sea side of the WAIS.

Finally, our results further support the use of the WAIS Divide ice-core record to assess past atmospheric conditions across the wider Western Divide and even a substantial portion of the WAIS, making it a powerful dataset for ice-sheet models. The higher mid-Holocene accumulation estimates compared to modern reportedinferred here over large sectors of the WAIS occurred at a time of sustained, millennial-scale increase in accumulation rates found at the WAIS Divide Ice Core. This pattern indicates that the ice core is suitably representative of the climatic conditions of the wider region over time. We suggest that future regional or continental ice-sheet modelling studies base their palaeoclimate forcing on modern spatial SMB products that are modulated over time using the WAIS Divide Ice Core record. This will enable those models to obtain a more realistic climatic forcing representative of the past conditions of the wider WAIS, and ultimately, constrain ice-sheet volume change and grounding-line evolution during the Holocene. The higher accumulation rates reported here occurred at a time of asynchronous grounding-line migration over the WAIS, including re-advances of the grounding-line in the Weddell and Ross sectors and evidence for delayed deglaciation in the Weddell Sea side of the WAIS. We suggest that ice-sheet model account for the evolution of accumulation rates over time when predicting past and future sea level coming from West Antarctica instead of using a fixed Last Glacial Maximum value.

Code availability

All the codes used to produce the results presented in this paper will be made available on the GitHub page of Julien A. Bodart (https://github.com/julbod, last accessed: 15 October 2022) and on Zenodo (Bodart et al., 2023a) upon acceptance of this manuscript.

Data availability

The IRH information for each of the three surveys used in this paper are archived in open-access repositories (Ashmore et al., 2020b; Bodart et al., 2021b; UTIG R1 layer to be made available via USAP-DC in due course) with references and links provided in the reference list. The BAS airborne radar data which were used to extract the IRHs used in this paper are fully available at the UK Polar Data Centre via the Polar Airborne Geophysics Data Portal (see Fremand, Bodart et al., 2022). The full RACMO-2.3p2 product is available on request from j.m.vanwessem@uu.nl or m.r.vandenbroeke@uu.nl. Links to access the observational point-based datasets used here are available from the respective references mentioned in the text (Section 2.4). The gridded depth and accumulation output from this study will be archived on Zenodo at the UK Polar Data Centre upon acceptance of this manuscript (Bodart et al., 2023b).

Author contribution

J.A.B. designed the study with supervision from R.G.B., D.A.Y., and D.D.B. J.A.B performed the data processing, gridding, and 1-D modelling, with contributions from J.A.M. for the modelling approach. J.A.B. interpreted the results with input from R.G.B., D.A.Y., D.D.B., and J.A.M. J.A.B. wrote the paper, with edits from R.G.B., D.A.Y., J.A.M., D.W.A., E.Q., A.S.H., D.G.V., D.D.B.all co-authors.

Competing interests

The authors declare that they have no conflict of interest.

Acknowledgments

The authors would like to dedicate this work to our dear friend and colleague, Professor David Vaughan, who recently passed away. This study was motivated by the AntArchitecture SCAR Action Group. UTIG acknowledges- the high school students who did the original AGASEA layer interpretation.

Financial support

J.A.B. was supported by the NERC Doctoral Training Partnership grant (NE/L002558/1), hosted in the Edinburgh E[3] DTP programme~~program~~. J.A.B. also acknowledges the Scottish Alliance for Geoscience, Environment and Society (SAGES) for funding a Postdoctoral and Early Career Researcher Exchanges scheme to UTIG. Support for UTIG data analysis was received from NSF grant nos CDI-0941678, PLR-1443690, and PLR-10437661, as well as the G. Unger Vetlesen Foundation and the UTIG Gale White and Ewing/Worzel Fellowships. This is UTIG contribution number: xxxx (TBD).

References

Arndt, J.E., Hillenbrand, C.D., Grobe, H., Kuhn, G. and Wacker, L.: Evidence for a dynamic grounding line in outer Filchner Trough, Antarctica, until the early Holocene, Geology, 45(11), 1035-1038, https://doi.org/10.1130/G39398.1, 2017.

Ashmore, D.W., Bingham, R.G., Ross, N., Siegert, M.J., Jordan, T.A. and Mair, D.W.: Englacial architecture and age-depth constraints across the West Antarctic Ice Sheet, Geophys. Res. Lett., 47 (6), p.e2019GL086663, https://doi.org/10.1029/2019GL086663, 2020a.

Ashmore, D.W., Bingham, R.G., Ross, N., Siegert, M., Jordan, T.A. and Mair, D.W.F.:. Radiostratigraphy of the Weddell Sea sector of West Antarctica, v2.0.0, Zenodo [data set], https://doi.org/10.5281/zenodo.4945301, 2020b.

Balco, G., Brown, N., Nichols, K., Venturelli, R.A., Adams, J., Braddock, S., Campbell, S., Goehring, B., Johnson, J.S., Rood, D.H. and Wilcken, K.: Reversible ice sheet thinning in the Amundsen Sea Embayment during the Late Holocene, The Cryosphere Discussions, pp.1-24, https://doi.org/10.5194/tc-2022-172, 2022.

Beem, L.H., Young, D.A., Greenbaum, J.S., Blankenship, D.D., Cavitte, M.G., Guo, J. and Bo, S.: Aerogeophysical characterization of Titan Dome, East Antarctica, and potential as an ice core target, The Cryosphere, 15 (4), 1719-1730, https://doi.org/10.5194/tc-15-1719-2021, 2021.

Bingham, R.G. and Siegert, M.J.: Radio-echo sounding over polar ice masses. J Environ. Eng. Geoph., 12 (1), https://doi.org/10.2113/JEEG12.1.47, 47-62, 2007.

Bracegirdle, T.J., Colleoni, F., Abram, N.J., Bertler, N.A., Dixon, D.A., England, M., Favier, V., Fogwill, C.J., Fyfe, J.C., Goodwin, I. and Goosse, H.: Back to the future: Using long-term observational and palaeo-proxy reconstructions to improve model projections of Antarctic climate, Geosci. J., 9 (6), 255, https://doi.org/10.3390/geosciences9060255, 2019.

Braddock, S., Hall, B.L., Johnson, J.S., Balco, G., Spoth, M., Whitehouse, P.L., Campbell, S., Goehring, B.M., Rood, D.H. and Woodward, J.: Relative sea-level data preclude major late Holocene ice-mass change in Pine Island Bay, Nat. Geosci., 15, 568-572, https://doi.org/10.1038/s41561-022-00961-y, 2022.

Bradley, S.L., Hindmarsh, R.C., Whitehouse, P.L., Bentley, M.J. and King, M.A.: Low post-glacial rebound rates in the Weddell Sea due to Late Holocene ice-sheet readvance, Earth Planet. Sc. Lett., 413, 79-89, https://doi.org/10.1016/j.epsl.2014.12.039, 2015.

Bodart, J. A., Bingham, R. G., Ashmore, D. W., Karlsson, N.B., Hein, A. S., and Vaughan, D. G.: Age-depth stratigraphy of Pine Island Glacier inferred from airborne radar and ice core chronology, J. Geophys. Res.-Earth, 126, e2020JF005927, https://doi.org/10.1029/2020JF005927, 2021a.

Bodart, J.A., Bingham, R.G., Ashmore, D.W., Karlsson, N.B., Hein, A.S., and Vaughan, D.G.: Dated radar stratigraphy of the Pine Island Glacier catchment (West Antarctica) derived from BBAS-PASIN (2004-05) and OIB-MCoRDS2 (2016/2018) surveys, v.1.0.0, UK Polar Data Centre, Natural Environment Research Council, UK Research and Innovation [data set], https://doi.org/10.5285/F2DE31AF-9F83-44F8-9584-F0190A2CC3EB, 2021b.

~~Bodart, J.A..: Calculate WAIS Holocene accumulation from airborne radar reflector, v.1.0.0., Zenodo [code], doi TBD, 2023a.~~

Bodart, J.A., Bingham, R.G., Young, D.A., MacGregor, J.M., Ashmore, D.W., Quartini, E., Vaughan, D.G., and Blankenship D.D.: Gridded depth and accumulation~~ and depth~~ products from dated airborne radar stratigraphy over West Antarctica during the mid-Holocene, v.1.0.0, ~~UK Polar Data Centre, Natural Environment Research Council, UK Research and Innovation~~Zenodo [data set], doi TBD, 2023~~b~~.

Buizert, C., Fudge, T.J., Roberts, W.H., Steig, E.J., Sherriff-Tadano, S., Ritz, C., Lefebvre, E., Edwards, J., Kawamura, K., Oyabu, I. and Motoyama, H.: Antarctic surface temperature and elevation during the Last Glacial Maximum, Science, 372 (6546), 1097-1101, https://doi.org/10.1126/science.abd2897, 2021.

Burgener, L., Rupper, S., Koenig, L., Forster, R., Christensen, W.F., Williams, J., Koutnik, M., Miege, C., Steig, E.J., Tingey, D. and Keeler, D.: An observed negative trend in West Antarctic accumulation rates from 1975 to 2010: Evidence from new observed and simulated records. J. Geophys. Res.-Atmos., 118 (10), 4205-4216, https://doi.org/10.1002/jgrd.50362, 2013.

Cavitte, M.G., Blankenship, D.D., Young, D.A., Schroeder, D.M., Parrenin, F., Lemeur, E., Macgregor, J.A. and Siegert, M.J.: Deep radiostratigraphy of the East Antarctic plateau: connecting the Dome C and Vostok ice core sites, J. Glaciol., 62 (232), 323-334, https://doi.org/10.1017/jog.2016.11, 2016.

Cavitte, M.G., Parrenin, F., Ritz, C., Young, D.A., Liefferinge, B., Blankenship, D.D., Frezzotti, M. and Roberts, J.: Accumulation patterns around Dome C, East Antarctica, in the last 73 kyr, The Cryosphere, 12, pp.1401-1414. doi: 10.5194/tc-12-1401-2018, 2018.

Cavitte, M.G., Goosse, H., Wauthy, S., Kausch, T., Tison, J.L., Van Liefferinge, B., Pattyn, F., Lenaerts, J.T. and Claeys, P.: From ice core to ground-penetrating radar: representativeness of SMB at three ice rises along the Princess Ragnhild Coast, East Antarctica, J. Glaciol., 68(272), pp.1221-1233, https://doi.org/10.1017/jog.2022.39, 2022.

Chavaillaz, Y., Codron, F. and Kageyama, M.: Southern westerlies in LGM and future (RCP4. 5) climates, Clim. Past, 9 (2), 517-524, https://doi.org/10.5194/cp-9-517-2013, 2013.

~~Cuffey, K.M., Clow, G.D., Steig, E.J., Buizert, C., Fudge, T.J., Koutnik, M., Waddington, E.D., Alley, R.B. and Severinghaus, J.P.: Deglacial temperature history of West Antarctica, P. Natl. A. Sci., 113 (50), 14249-14254, https://doi.org/10.1073/pnas.1609132113, 2016.~~

Cole-Dai, J., Ferris, D.G., Kennedy, J.A., Sigl, M., McConnell, J.R., Fudge, T.J., Geng, L., Maselli, O.J., Taylor, K.C. and Souney, J.M.: Comprehensive record of volcanic eruptions in the Holocene (11,000 years) from the WAIS Divide, Antarctica ice core, J. Geophys. Res.-Atmos., 126 (7), p.e2020JD032855, https://doi.org/10.1029/2020JD032855, 2021.

Corr, H.F., Ferraccioli, F., Frearson, N., Jordan, T., Robinson, C., Armadillo, E., Caneva, G., Bozzo, E. and Tabacco, I.: Airborne radio-echo sounding of the Wilkes Subglacial Basin, the Transantarctic Mountains and the Dome C region, Terra Ant. Rep., 13, pp.55-63. https://nora.nerc.ac.uk/id/eprint/13578 (last access: 15 October 2022), 2007.

CReSIS: CReSIS Radar Depth Sounder Data, Lawrence, Kansas, USA. Digital Media. http://data.cresis.ku.edu/ (last access: 15 October 2022), 2018.

Dansgaard, W. and Johnsen, S. J.: A flow model and a time scale for the ice core from Camp Century, Greenland, J. Glacio., 8 (53), 215–223, https://doi.org/10.3189/S0022143000031208, 1969.

Dattler, M.E., Lenaerts, J.T. and Medley, B.: Significant spatial variability in radar-derived west Antarctic accumulation linked to surface winds and topography, Geophys. Res. Lett., 46(22), pp.13126-13134, https://doi.org/10.1029/2019GL085363, 2019.

DeConto, R.M. and Pollard, D.: Contribution of Antarctica to past and future sea-level rise, Nature, 531 (7596), 591-597, https://doi.org/10.1038/nature17145, 2016.

Denton, G.H. and Hughes, T.J.: Reconstructing the Antarctic ice sheet at the Last Glacial Maximum, Quaternary Sci. Rev., 21 (1-3), 193-202, https://doi.org/10.1016/S0277-3791(01)00090-7, 2002.

Fahnestock, M., Abdalati, W., Joughin, I., Brozena, J. and Gogineni, P.: High geoSthermal heat flow, basal melt, and the origin of rapid ice flow in central Greenland, Science, 294 (5550), 2338-2342, https://doi.org/10.1126/science.1065370, 2001a.

Fahnestock, M., Abdalati, W., Luo, S. and Gogineni, S.: Internal layer tracing and age-depth-accumulation relationships for the northern Greenland ice sheet, J. Geophys. Res.-Atmos, 106(D24), pp.33789-33797, https://doi.org/10.1029/2001JD900200, 2001b.

Favier, V., Agosta, C., Parouty, S., Durand, G., Delaygue, G., Gallée, H., Drouet, A.-S., Trouvilliez, A., and Krinner, G.: An updated and quality controlled surface mass balance dataset for Antarctica, The Cryosphere, 7, 583-597, https://doi.org/10.5194/tc-7-583-2013, 2013.

Frémand, A.C., Bodart, J.A., Jordan, T.A., Ferraccioli, F., Robinson, C., Corr, H.F., Peat, H.J., Bingham, R.G. and Vaughan, D.G.: British Antarctic Survey's Aerogeophysical Data: Releasing 25 Years of Airborne Gravity, Magnetic, and Radar Datasets over Antarctica, Earth Syst. Sci. Data, 14, 3379–3410, https://doi.org/10.5194/essd-14-3379-2022, 2022.

Fudge, T.J., Markle, B.R., Cuffey, K.M., Buizert, C., Taylor, K.C., Steig, E.J., Waddington, E.D., Conway, H. and Koutnik, M.: Variable relationship between accumulation and temperature in West Antarctica for the past 31,000 years, Geophys. Res. Lett., 43(8), 3795-3803, https://doi.org/10.1002/2016GL068356, 2016.

Fudge, T. J., Buizert, C., Conway, H., and Waddington, E. D.: Accumulation Rates from the WAIS Divide Ice Core, v.1.0.0., U.S. Antarctic Program Data Center [data set], https://doi.org/10.15784/601004, 2017.

Golledge, N.R., Fogwill, C.J., Mackintosh, A.N. and Buckley, K.M.: Dynamics of the last glacial maximum Antarctic ice-sheet and its response to ocean forcing, P. Natl. Acad. Sci., 109(40), pp.16052-16056, https://doi.org/10.1073/pnas.1205385109, 2012.

Golledge, N.R., Levy, R.H., McKay, R.M., Fogwill, C.J., White, D.A., Graham, A.G., Smith, J.A., Hillenbrand, C.D., Licht, K.J., Denton, G.H. and Ackert Jr, R.P.: Glaciology and geological signature of the Last Glacial Maximum Antarctic ice sheet, Quaternary Sci. Rev., 78, pp.225-247, https://doi.org/10.1016/j.quascirev.2013.08.011, 2013

Haran, T., M. Klinger, J. Bohlander, M. Fahnestock, T. Painter, and T. Scambos: MEaSUREs MODIS Mosaic of Antarctica 2013-2014 (MOA2014) Image Map, v.1.0.0., NASA National Snow and Ice Data Center Distributed Active Archive Center [data set], https://doi.org/10.5067/RNF17BP824UM, 2018.

Harrison, C. H.: Radio Echo Sounding of Horizontal Layers in Ice, J. Glaciol., 12, 66, 383–397, https://doi.org/10.3189/S0022143000031804, 1973.

Hein, A.S., Marrero, S.M., Woodward, J., Dunning, S.A., Winter, K., Westoby, M.J., Freeman, S.P., Shanks, R.P. and Sugden, D.E.: Mid-Holocene pulse of thinning in the Weddell Sea sector of the West Antarctic ice sheet, Nat. Commun., 7 (1), 1-8, https://doi.org/10.1038/ncomms12511, 2016.

Hillenbrand, C.D., Kuhn, G., Smith, J.A., Gohl, K., Graham, A.G., Larter, R.D., Klages, J.P., Downey, R., Moreton, S.G., Forwick, M. and Vaughan, D.G.: Grounding-line retreat of the west Antarctic ice sheet from inner Pine island Bay, Geology, 41 (1), 35-38, https://doi.org/10.1130/G33469.1, 2013.

Hillenbrand, C.D., Bentley, M.J., Stolldorf, T.D., Hein, A.S., Kuhn, G., Graham, A.G., Fogwill, C.J., Kristoffersen, Y., Smith, J.A., Anderson, J.B. and Larter, R.D.: Reconstruction of changes in the Weddell Sea sector of the Antarctic Ice Sheet since the Last Glacial Maximum, Quaternary Sci. Rev., 100, 111-136, https://doi.org/10.1016/j.quascirev.2013.07.020, 2014.

Hillenbrand, C.D., Smith, J.A., Hodell, D.A., Greaves, M., Poole, C.R., Kender, S., Williams, M., Andersen, T.J., Jernas, P.E., Elderfield, H. and Klages, J.P.: West Antarctic Ice Sheet retreat driven by Holocene warm water incursions, Nature, 547 (7661), 43-48, https://doi.org/10.1038/nature22995, 2017.

Holschuh, N., Parizek, B.R., Alley, R.B. and Anandakrishnan, S.: Decoding ice sheet behavior using englacial layer slopes, Geophys. Res. Lett., 44(11), pp.5561-5570, https://doi.org/10.1002/2017GL073417, 2017.

Holt, J. W., Blankenship, D. D., Morse, D. L., Young, D. A., Peters, M. E., Kempf, S. D., Richter, T. G., Vaughan, D. G., and Corr, H. F.: New boundary conditions for the West Antarctic Ice Sheet: Subglacial topography of the Thwaites and Smith glacier catchments, Geophys. Res. Lett., 33, L09502, https://doi.org/10.1029/2005GL025561, 2006.

IPCC: Climate Change 2021: The Physical Science Basis. Contribution of Working Group I to the Sixth Assessment Report of the Intergovernmental Panel on Climate Change, edited by: Masson-Delmotte, V., Zhai, P., Pirani, A., Connors, S. L., Péan, C., Berger, S., Caud, N., Chen, Y., Goldfarb, L., Gomis, M. I., Huang, M., Leitzell, K., Lonnoy, E., Matthews, J. B. R., Maycock, T. K., Waterfield, T., Yelekçi, O., Yu, R., and Zhou B., Cambridge University Press, Cambridge, United Kingdom and New York, NY, USA, 147–286, https://doi.org/10.1017/9781009157896.003, in press, 2021.

Jacobel, R. W., and Welch, B. C.: A time marker at 17.5 kyr BP detected throughout West Antarctica, Ann. Glaciol., 41, 47–51, https://doi.org/10.3189/172756405781813348, 2005.

Johnson, J.S., Bentley, M.J., Smith, J.A., Finkel, R.C., Rood, D.H., Gohl, K., Balco, G., Larter, R.D. and Schaefer, J.M.: Rapid thinning of Pine Island Glacier in the early Holocene, Science, 343 (6174), 999-1001, https://doi.org/10.1126/science.1247385, 2014.

Johnson, J.S., Roberts, S.J., Rood, D.H., Pollard, D., Schaefer, J.M., Whitehouse, P.L., Ireland, L.C., Lamp, J.L., Goehring, B.M., Rand, C. and Smith, J.A.: Deglaciation of Pope Glacier implies widespread early Holocene ice sheet thinning in the Amundsen Sea sector of Antarctica, Earth Planet Sc. Lett., 548, p.116501, https://doi.org/10.1016/j.epsl.2020.116501, 2020.

Johnson, J.S., Pollard, D., Whitehouse, P.L., Roberts, S.J., Rood, D.H. and Schaefer, J.M.: Comparing glacial-geological evidence and model simulations of ice sheet change since the last glacial period in the Amundsen Sea sector of Antarctica, J. Geophys. Res.-Earth, 126(6), p.e2020JF005827, https://doi.org/10.1029/2020JF005827, 2021.

Johnson, J.S., Venturelli, R.A., Balco, G., Allen, C.S., Braddock, S., Campbell, S., Goehring, B.M., Hall, B.L., Neff, P.D., Nichols, K.A. and Rood, D.H.: Existing and potential evidence for Holocene grounding line retreat and readvance in Antarctica, The Cryosphere, 16 (5), 1543-1562, https://doi.org/10.5194/tc-16-1543-2022, 2022.

Jones, R.S., Johnson, J.S., Lin, Y., Mackintosh, A.N., Sefton, J.P., Smith, J.A., Thomas, E.R. and Whitehouse, P.L.: Stability of the Antarctic Ice Sheet during the pre-industrial Holocene, Nat. Rev. Earth Environ., 3, 500-515, https://doi.org/10.1038/s43017-022-00309-5, 2022.

Karlsson, N. B., Bingham, R. G., Rippin, D. M., Hindmarsh, R. C., Corr, H. F., and Vaughan, D. G.: Constraining past accumulation in the central Pine Island Glacier basin, West Antarctica, using radio-echo sounding, J. Glaciol., 60, 553–562, https://doi.org/10.3189/2014JoG13j180, 2014.

Kausch, T., Lhermitte, S., Lenaerts, J., Wever, N., Inoue, M., Pattyn, F., Sun, S., Wauthy, S., Tison, J.L. and Van De Berg, W.J.: Impact of coastal East Antarctic ice rises on surface mass balance: insights from observations and modeling, The Cryosphere, 14(10), pp.3367-3380, https://doi.org/10.5194/tc-14-3367-2020, 2020.

Kingslake, J., Scherer, R.P., Albrecht, T., Coenen, J., Powell, R.D., Reese, R., Stansell, N.D., Tulaczyk, S., Wearing, M.G. and Whitehouse, P.L.: Extensive retreat and re-advance of the West Antarctic Ice Sheet during the Holocene, Nature, 558 (7710), 430-434, https://doi.org/10.1038/s41586-018-0208-x, 2018.

Koutnik, M.R., Fudge, T.J., Conway, H., Waddington, E.D., Neumann, T.A., Cuffey, K.M., Buizert, C. and Taylor, K.C.: Holocene accumulation and ice flow near the West Antarctic Ice Sheet Divide ice core site, J. Geophys. Res.-Earth, 121 (5), 907-924. https://doi.org/10.1002/2015JF003668, 2016.

Kurbatov, A.V., Zielinski, G.A., Dunbar, N.W., Mayewski, P.A., Meyerson, E.A., Sneed, S.B. and Taylor, K.C.: A 12,000 year record of explosive volcanism in the Siple Dome Ice Core, West Antarctica, J. Geophys. Res.-Atmos, 111 (D12). https://doi.org/10.1029/2005JD006072, 2006.

Le Brocq, A.M., Bentley, M.J., Hubbard, A., Fogwill, C.J., Sugden, D.E. and Whitehouse, P.L.: Reconstructing the Last Glacial Maximum ice sheet in the Weddell Sea embayment, Antarctica, using numerical modelling constrained by field evidence, Quaternary Sci. Rev., 30(19-20), pp.2422-2432, https://doi.org/10.1016/j.quascirev.2011.05.009, 2011.

Leysinger Vieli, G.J.M., Siegert, M.J. and Payne, A.J.: Reconstructing ice-sheet accumulation rates at ridge B, East Antarctica, Ann. Glaciol., 39, pp.326-330, https://doi.org/10.3189/172756404781814519, 2004.

Leysinger Vieli, G.J.M., Hindmarsh, R.C., Siegert, M.J. and Bo, S.: Time-dependence of the spatial pattern of accumulation rate in East Antarctica deduced from isochronic radar layers using a 3-D numerical ice flow model, J. Geophys. Res.-Earth, 116 (F2), F02018, https://doi.org/10.1029/2010JF001785, 2011.

Leysinger Vieli, G.M., Martin, C., Hindmarsh, R.C.A. and Lüthi, M.P., Basal freeze-on generates complex ice-sheet stratigraphy, Nat. Commun., 9(1), p.4669, https://doi.org/10.1038/s41467-018-07083-3, 2018.

MacGregor, J.A., Matsuoka, K., Koutnik, M.R., Waddington, E.D., Studinger, M. and Winebrenner, D.P.: Millennially averaged accumulation rates for the Vostok Subglacial Lake region inferred from deep internal layers, Ann. Glaciol., 50 (51), 25-34. https://doi.org/10.3189/172756409789097441, 2009.

MacGregor, J.A., Catania, G.A., Conway, H., Schroeder, D.M., Joughin, I., Young, D.A., Kempf, S.D. and Blankenship, D.D.: Weak bed control of the eastern shear margin of Thwaites Glacier, West Antarctica, J. Glaciol., 59 (217), 900-912, https://doi.org/10.3189/2013JoG13J050, 2013.

MacGregor, J. A., Colgan, W. T., Fahnestock, M. A., Morlighem, M., Catania, G. A., Paden, J. D., and Gogineni, S. P.: Holocene deceleration of the Greenland ice sheet, Science, 351 (6273), 590–593, https://doi.org/10.1126/science.aab1702, 2016.

MacGregor, J. A., Boisvert, L. N., Medley, B., Petty, A. A., Harbeck, J. P., Bell, R. E., Blair, J. B., Blanchard-Wrigglesworth, E., Buckley, E.,M., Christoffersen, M. S., and Cochran, J. R.: The scientific legacy of NASA's Operation Icebridge, Rev. Geophys., 59, e2020RG000712, https://doi.org/10.1029/2020RG000712, 2021.

Mayewski, P. A. and Dixon, D.A: US International TransAntarctic Scientific Expedition (US ITASE) Glaciochemical Data, v. 2.0.0., NASA National Snow and Ice Data Center [data set], http://dx.doi.org/10.7265/N51V5BXR, 2013.

~~McConnell, J.R., Burke, A., Dunbar, N.W., Köhler, P., Thomas, J.L., Arienzo, M.M., Chellman, N.J., Maselli, O.J., Sigl, M., Adkins, J.F. and Baggenstos, D.: Synchronous volcanic eruptions and abrupt climate change~ 17.7 ka plausibly linked by stratospheric ozone depletion, P. Natl. A. Sci., 114 (38), 10035-10040, https://doi.org/10.1073/pnas.1705595114, 2017.~~

Medley, B., Joughin, I., Das, S.B., Steig, E.J., Conway, H., Gogineni, S., Criscitiello, A.S., McConnell, J.R., Smith, B.E., van den Broeke, M.R. and Lenaerts, J.T.: Airborne-radar and ice-core observations of annual snow accumulation over Thwaites Glacier, West Antarctica confirm the spatiotemporal variability of global and regional atmospheric models, Geophys. Res. Lett., 40(14), pp.3649-3654, https://doi.org/10.1002/grl.50706, 2013.

Medley, B., Joughin, I., Smith, B.E., Das, S.B., Steig, E.J., Conway, H., Gogineni, S., Lewis, C., Criscitiello, A.S., McConnell, J.R. and van den Broeke, M.R.: Constraining the recent mass balance of Pine Island and Thwaites glaciers, West Antarctica, with airborne observations of snow accumulation, The Cryosphere, 8 (4), 1375-1392, https://doi.org/10.5194/tc-8-1375-2014, 2014.

Morlighem, M.: MEaSUREs BedMachine Antarctica, v.2.0.0., NASA National Snow and Ice Data Center Distributed Active Archive Center [data set], https://doi.org/10.5067/E1QL9HFQ7A8M, 2020.

Mouginot, J., Scheuchl, B., and Rignot., E.: MEaSUREs Antarctic Boundaries for IPY 2007-2009 from Satellite Radar, v.2.0.0., NASA National Snow and Ice Data Center Distributed Active Archive Center [data set], http://dx.doi.org/10.5067/AXE4121732AD, 2017.

Muldoon, G. R., Jackson, C. S., Young, D. A., and Blankenship, D. D.: Bayesian estimation of englacial radar chronology in Central West Antarctica, Dynamics and Statistics of the Climate System, 3(1), dzy004, https://doi.org/10.1093/climatesystem/dzy004, 2018.

Neuhaus, S.U., Tulaczyk, S.M., Stansell, N.D., Coenen, J.J., Scherer, R.P., Mikucki, J.A. and Powell, R.D.: Did Holocene climate changes drive West Antarctic grounding line retreat and readvance?, The Cryosphere, 15(10), 4655-4673, https://doi.org/10.5194/tc-15-4655-2021, 2021.

Neumann, T. A., Conway, H., Price, S. F., Waddington, E. D., Catania, G. A., and Morse, D. L.: Holocene accumulation and ice sheet dynamics in central West Antarctica, J. Geophys. Res.-Earth, 113 (F2), F02018, https://doi.org/10.1029/2007JF000764, 2008.

Nichols, K.A., Goehring, B.M., Balco, G., Johnson, J.S., Hein, A.S. and Todd, C.: New last glacial maximum ice thickness constraints for the Weddell Sea Embayment, Antarctica, The Cryosphere, 13(11), 2935-2951, https://doi.org/10.5194/tc-13-2935-2019, 2019.

Nielsen, L.T., Karlsson, N.B. and Hvidberg, C.S.: Large-scale reconstruction of accumulation rates in northern Greenland from radar data, Ann. Glaciol., 56(70), pp.70-78 https://doi.org/10.3189/2015AoG70A062, 2015.

Nye, J. F.: The distribution of stress and velocity in glaciers and ice-sheets, P. Roy. Soc. Lond. A. Mat., 239 (1216), 113–133. https://doi.org/10.1098/rspa.1957.0026, 1957.

Parrenin, F., Barnola, J.M., Beer, J., Blunier, T., Castellano, E., Chappellaz, J., Dreyfus, G., Fischer, H., Fujita, S., Jouzel, J. and Kawamura, K.: The EDC3 chronology for the EPICA Dome C ice core, Clim. Past, 3(3), pp.485-497, https://doi.org/10.5194/cp-3-485-2007, 2007.

Peters, M.E., Blankenship, D.D., Carter, S.P., Kempf, S.D., Young, D.A. and Holt, J.W.: Along-track focusing of airborne radar sounding data from West Antarctica for improving basal reflection analysis and layer detection, IEEE T. Geosci. Remote., https://doi.org/10.1109/TGRS.2007.897416, 45 (9), 2725-2736, 2007.

Petit, J.R., Jouzel, J., Raynaud, D., Barkov, N.I., Barnola, J.M., Basile, I., Bender, M., Chappellaz, J., Davis, M., Delaygue, G. and Delmotte, M.: Climate and atmospheric history of the past 420,000 years from the Vostok ice core, Antarctica, Nature, 399(6735), pp.429-436, https://doi.org/10.1038/20859, 1999.

Rignot, E., Mouginot, J., and Scheuchl, B.: MEaSUREs InSAR-based Antarctica ice velocity map, v.2.0.0., NASA National Snow and Ice Data Center Distributed Active Archive Center [data set], https://doi.org/10.5067/D7GK8F5J8M8R, 2017.

Ross, N., Siegert, M.J., Woodward, J., Smith, A.M., Corr, H.F., Bentley, M.J., Hindmarsh, R.C., King, E.C. and Rivera, A.: Holocene stability of the Amundsen-Weddell ice divide, West Antarctica, Geology, 39 (10), 935-938, https://doi.org/10.1130/G31920.1, 2011.

Ross, N., Bingham, R.G., Corr, H.F., Ferraccioli, F., Jordan, T.A., Le Brocq, A., Rippin, D.M., Young, D., Blankenship, D.D. and Siegert, M.J.: Steep reverse bed slope at the grounding line of the Weddell Sea sector in West Antarctica, Nat. Geosci., 5 (6), 393-396, https://doi.org/10.1038/ngeo1468, 2012.

Siegert, M.J. and Payne, A.J.: Past rates of accumulation in central West Antarctica, Geophys. Res. Lett., 31 (12), https://doi.org/10.1029/2004GL020290, 2004.

Siegert, M., Ross, N., Corr, H., Kingslake, J. and Hindmarsh, R.: Late Holocene ice-flow reconfiguration in the Weddell Sea sector of West Antarctica, Quaternary Sci. Rev., 78, 98-107, https://doi.org/10.1016/j.quascirev.2013.08.003, 2013.

Sigl, M., Toohey, M, McConnell, J.R., Cole-Dai, J., and Severi, M.: Volcanic stratospheric sulfur injections and aerosol optical depth during the Holocene (past 11 500 years) from a bipolar ice-core array, Earth Syst. Sci., 14, 3167–3196, https://doi.org/10.5194/essd-14-3167-2022, 2022.

Spector, P., Stone, J. and Goehring, B.: Thickness of the divide and flank of the West Antarctic Ice Sheet through the last deglaciation, The Cryosphere, 13 (11), 3061-3075, https://doi.org/10.5194/tc-13-3061-2019, 2019.

Sproson, A.D., Yokoyama, Y., Miyairi, Y., Aze, T. and Totten, R.L.: Holocene melting of the West Antarctic Ice Sheet driven by tropical Pacific warming, Nat. Commun., 13 (1), 1-9, https://doi.org/10.1038/s41467-022-30076-2, 2022.

Steig, E.J., Fastook, J.L., Zweck, C., Goodwin, I.D., Licht, K.J., White, J.W. and Ackert Jr, R.P.: West Antarctic ice sheet elevation changes, The West Antarctic Ice Sheet: Behavior and Environment, 77, 75-90. https://doi.org/10.1029/AR077p0075, 2001.

Stone, J.O., Balco, G.A., Sugden, D.E., Caffee, M.W., Sass III, L.C., Cowdery, S.G. and Siddoway, C.: Holocene deglaciation of Marie Byrd land, west Antarctica, Science, 299 (5603), 99-102, https://doi.org/10.1126/science.1077998, 2003.

Suganuma, Y., Miura, H., Zondervan, A. and Okuno, J.I.: East Antarctic deglaciation and the link to global cooling during the Quaternary: Evidence from glacial geomorphology and 10Be surface exposure dating of the Sør Rondane Mountains, Dronning Maud Land, Quaternary Sci. Rev., 97, pp.102-120, https://doi.org/10.1016/j.quascirev.2014.05.007, 2014.

Sutter, J., Fischer, H. and Eisen, O.: Investigating the internal structure of the Antarctic ice sheet: the utility of isochrones for spatiotemporal ice-sheet model calibration, The Cryosphere, 15 (8), 3839-3860. https://doi.org/10.5194/tc-15-3839-2021, 2021.

RAISED Consortium: A community-based geological reconstruction of Antarctic Ice Sheet deglaciation since the Last Glacial Maximum, Quaternary Sci. Rev., 100, pp.1-9, https://doi.org/10.1016/j.quascirev.2014.06.025, 2014.

vVan Den Broeke, M.R. and vVan Lipzig, N.P.: Changes in Antarctic temperature, wind and precipitation in response to the Antarctic Oscillation, Ann. Glaciol, 39, 119-126, https://doi.org/10.3189/172756404781814654, 2004.

Van Wessem, J.M., Van De Berg, W.J., Noël, B.P., Van Meijgaard, E., Amory, C., Birnbaum, G., Jakobs, C.L., Krüger, K., Lenaerts, J., Lhermitte, S. and Ligtenberg, S.R.: Modelling the climate and surface mass balance of polar ice sheets using RACMO2–Part 2: Antarctica (1979–2016), The Cryosphere, 12 (4), 479-1498, https://doi.org/10.5194/tc-12-1479-2018, 2018.

Vaughan, D.G., Corr, H.F., Ferraccioli, F., Frearson, N., O'Hare, A., Mach, D., Holt, J.W., Blankenship, D.D., Morse, D.L. and Young, D.A.: New boundary conditions for the West Antarctic ice sheet: Subglacial topography beneath Pine Island Glacier, Geophys. Res. Lett., 33 (9), L09501, https://doi.org/10.1029/2005GL025588, 2006.

Venturelli, R.A., Siegfried, M.R., Roush, K.A., Li, W., Burnett, J., Zook, R., Fricker, H.A., Priscu, J.C., Leventer, A. and Rosenheim, B.E.: Mid-Holocene grounding line retreat and readvance at Whillans Ice Stream, West Antarctica, Geophys. Res. Lett., 47 (15), p.e2020GL088476, https://doi.org/10.1029/2020GL088476, 2020.

Waddington, E. D., Neumann, T. A., Koutnik, M. R., Marshall, H.-P., and Morse, D. L.: Inference of accumulation-rate patterns from deep layers in glaciers and ice sheets, J. Glaciol., 53 (183), 694–712, https://doi.org/10.3189/002214307784409351, 2007.

WAIS Divide Project Members: Onset of deglacial warming in West Antarctica driven by local orbital forcing, Nature, 500 (7463), 440-444, https://doi.org/10.1038/nature12376, 2013.

Wearing, M.G. and Kingslake, J.: Holocene Formation of Henry Ice Rise, West Antarctica, Inferred from Ice-Penetrating Radar, J. Geophys. Res.-Earth, 124 (8), 2224-2240, https://doi.org/10.1029/2018JF004988, 2019.

Whillans, I. M.: Radio-echo layers and the recent stability of the West Antarctic ice sheet, Nature, 264, 5582, 152, https://doi.org/10.1038/264152a0, 1976.

Winter, A., Steinhage, D., Creyts, T.T., Kleiner, T. and Eisen, O.: Age stratigraphy in the East Antarctic Ice Sheet inferred from radio-echo sounding horizons, Earth Syst. Sci. Data, 11 (3), 1069-1081, https://doi.org/10.5194/essd-11-1069-2019, 2019.